Supplementary Information (SI) for Organic Chemistry Frontiers.

Unveiling stereoselective ladders via photo-oligomerization of a diazaanthracene macrocycle

Jinti Moni Kumar, [a] Ivan Huc, [b] Yann Ferrand, [c] and Bappaditya Gole*[a]

[a] Biomimetic Supramolecular Chemistry Laboratory, Department of Chemistry, School of Natural Sciences, Shiv Nadar Institution of Eminence Deemed to be University, Greater Noida, Uttar Pradesh 201314, India, E-mail: bappaditya.gole@snu.edu.in

[b] Department of Pharmacy, Ludwig-Maximilians-Universität München, Butenandtstr. 5–13, 81377 Munich (Germany)

[c] Univ. Bordeaux, CNRS, Bordeaux INP, CBMN, UMR 5248, F-33600 Pessac, France

Supporting Information

Table of contents

1. **Supporting schemes and figures**
2. **Material and methods**
3. **Methods for chemical synthesis**
4. **References**
5. **NMR Spectra**

1. Supporting schemes and figures

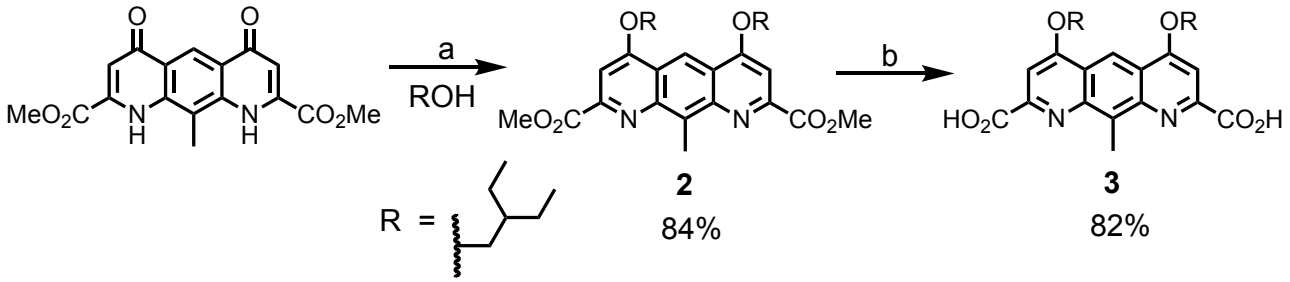

Scheme S1. (a) PPh_3, DIAD, dry THF, 16 hours, room temperature. (b) KOH, DCM/MeOH, 24 hours, room temperature.

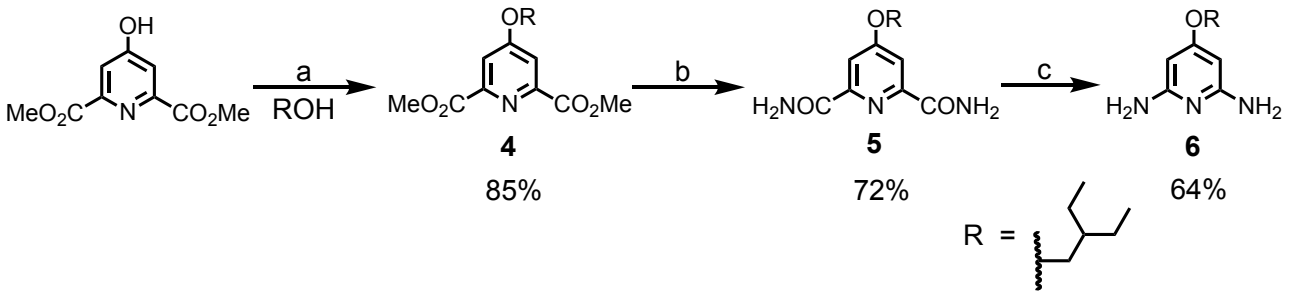

Scheme S2. (a) PPh_3, DIAD, dry THF, 18 hours, room temperature. (b) NH_3 gas, dry MeOH, 2 hours, R.T. (c) (i) KOH, Br_2, 0 °C, 1,4-dioxane, 10 min at 0 °C, 1 hour at 25 °C, 1.5 hours at 70 °C. (ii) Acetic acid.

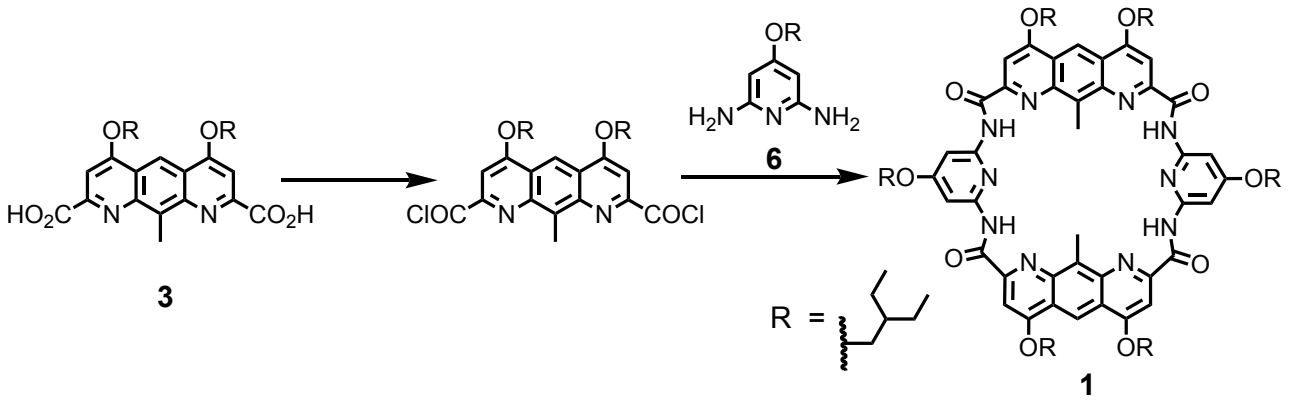

Scheme S3. (a) $(COCl)_2$, dry $CHCl_3$, 1.5 hours, room temperature. (b) DIPEA, dry THF, 18 hours, room temperature.

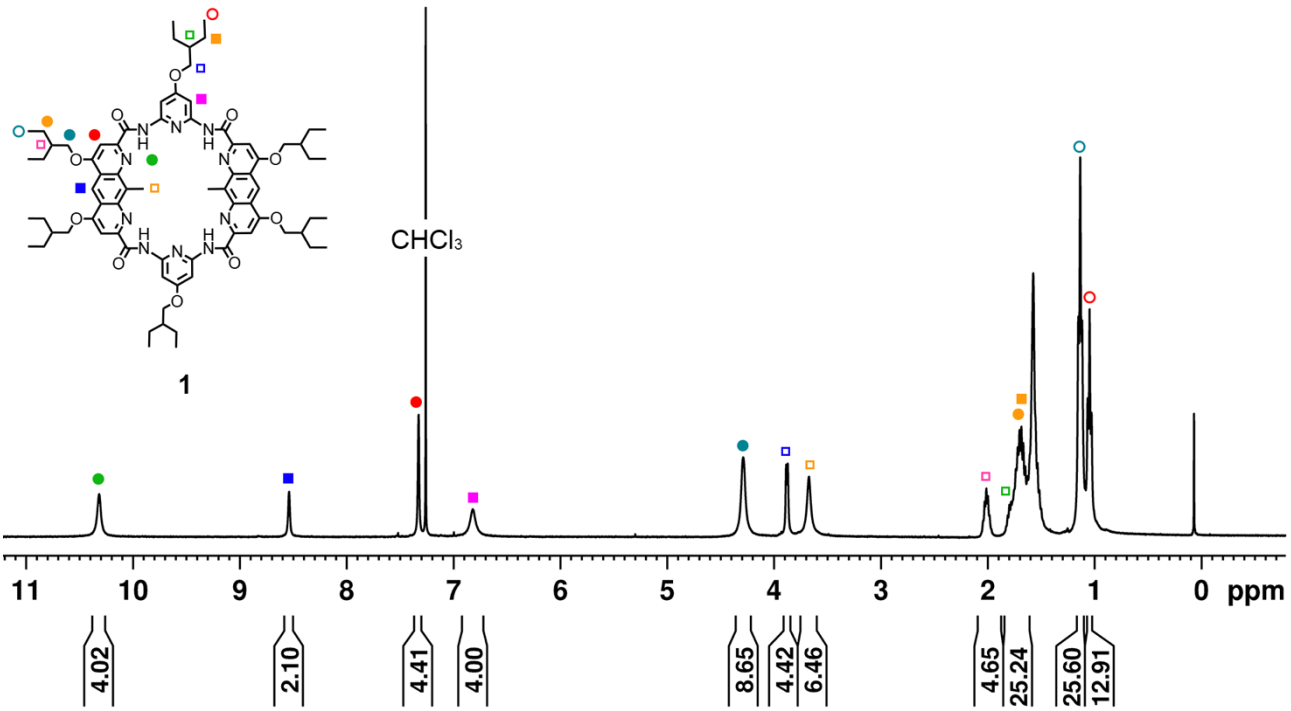

Fig. S1 400 MHz ^{1}H-NMR spectrum of **1** in $CDCl_3$ at 298 K.

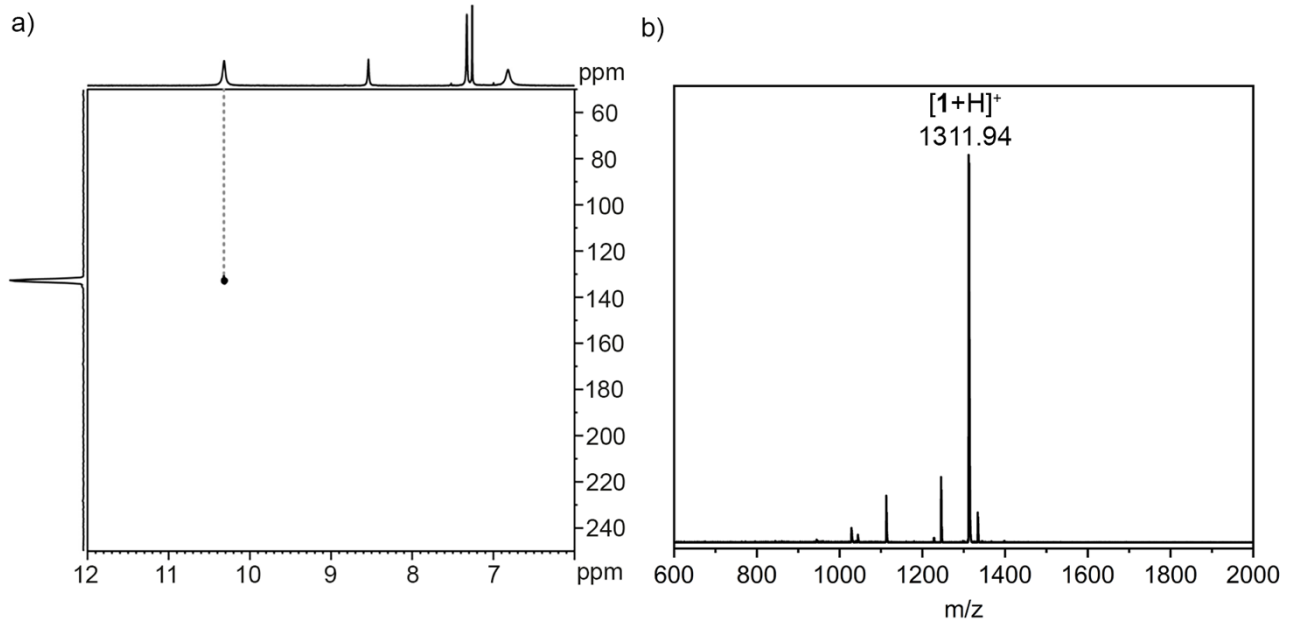

Fig. S2 (a) ^{15}N-^{1}H HSQC spectrum of **1** in $CDCl_3$ at 298 K identifying amide signals. (b) MALDI-TOF mass spectra of **1**. m/z calculated for $C_{76}H_{99}N_{10}O_{10}$ $[M+H]^+$ 1311.75, Found: 1311.94.

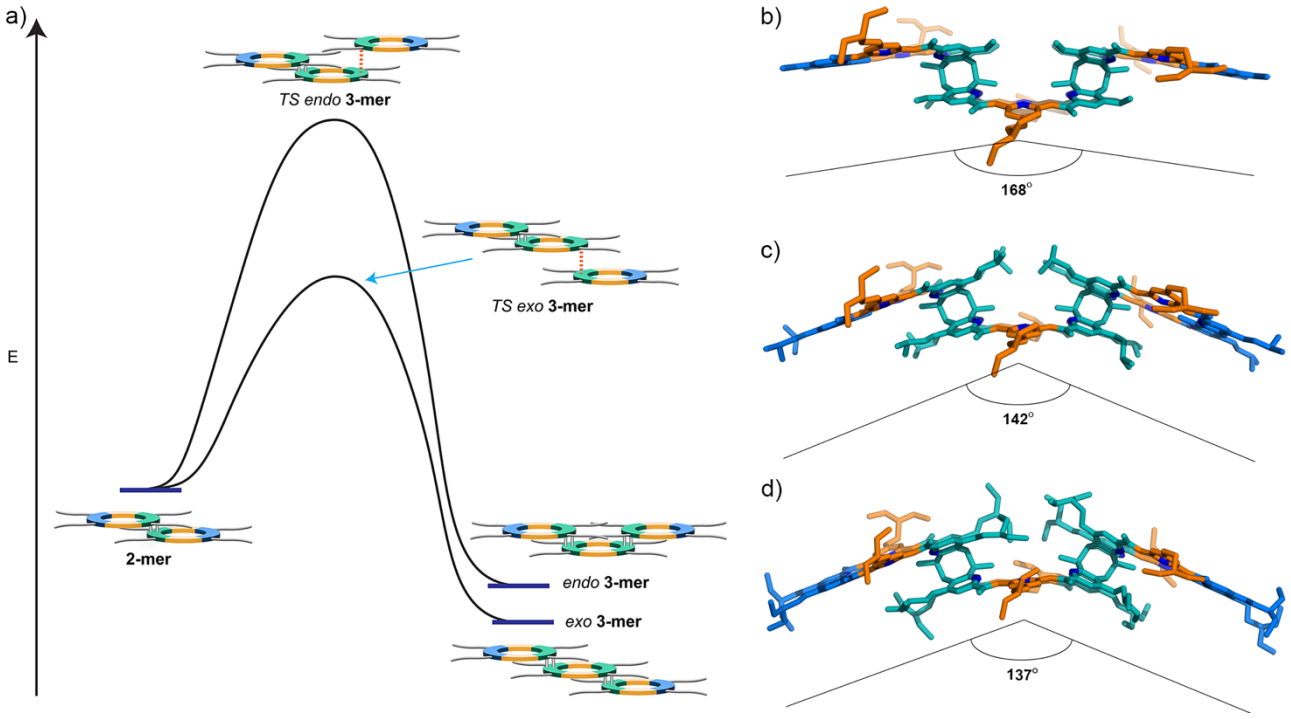

Fig. S3 a) Schematic presentation showing the expected higher transition state (TS) energy of *endo* **3-mer** compared to *exo* **3-mer** due to the steric hindrance between the approaching solubilizing side chains in the endo-isomer. This eventually facilitates the formation of *exo* **3-mer**. The geometry-optimized model using the Merck Molecular Force Field static (MMFFs) of the endo 3-mer with varying side chains of diazaanthracene: (a) methyl, (b) isobutyl, and (c) ethyl butyl. The bent angle of the terminal two units is given to highlight the strain on the central unit.

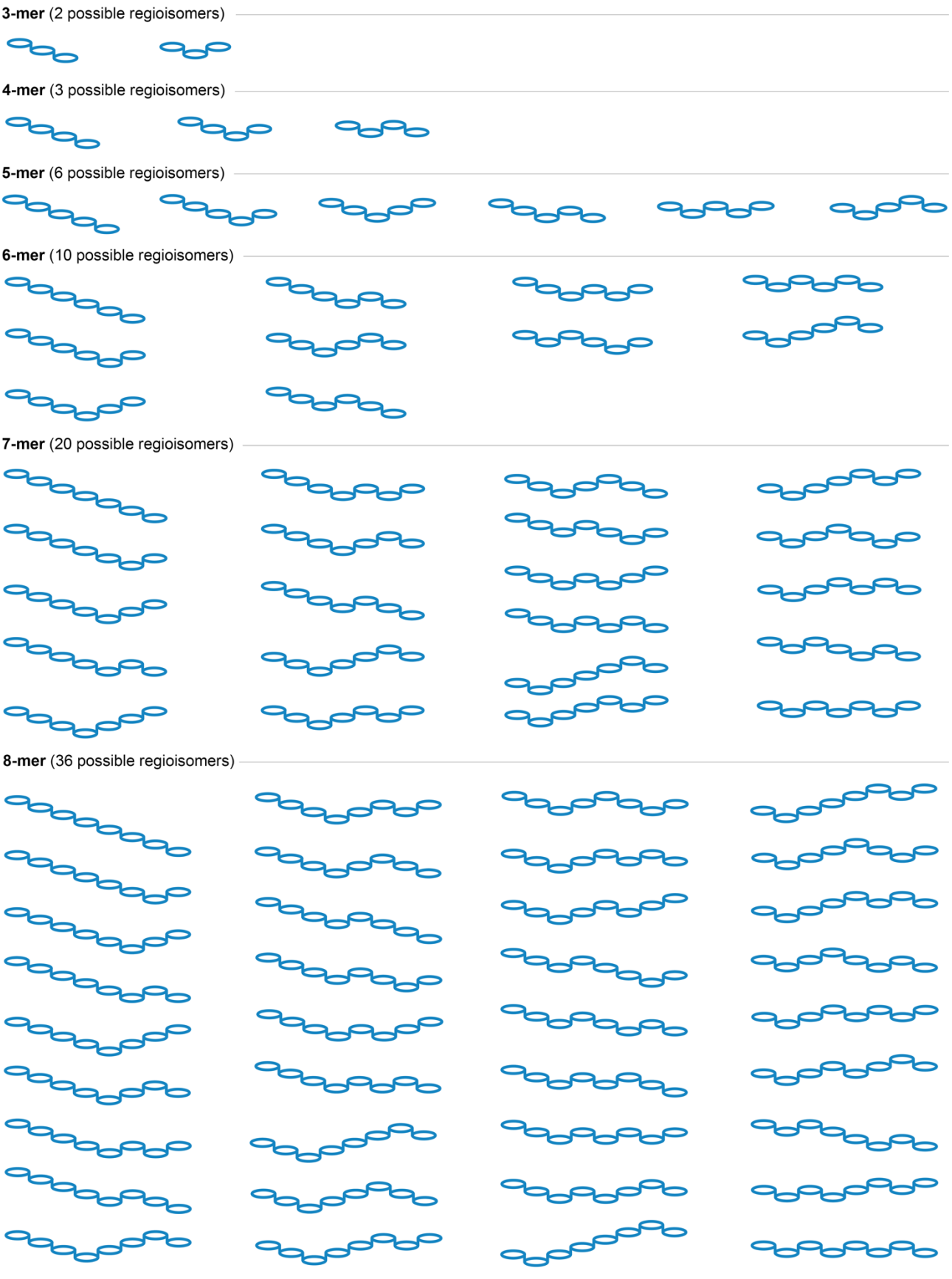

Fig. S4 Theoretical possible stereoisomers for **3-mer** to **8-mer**.

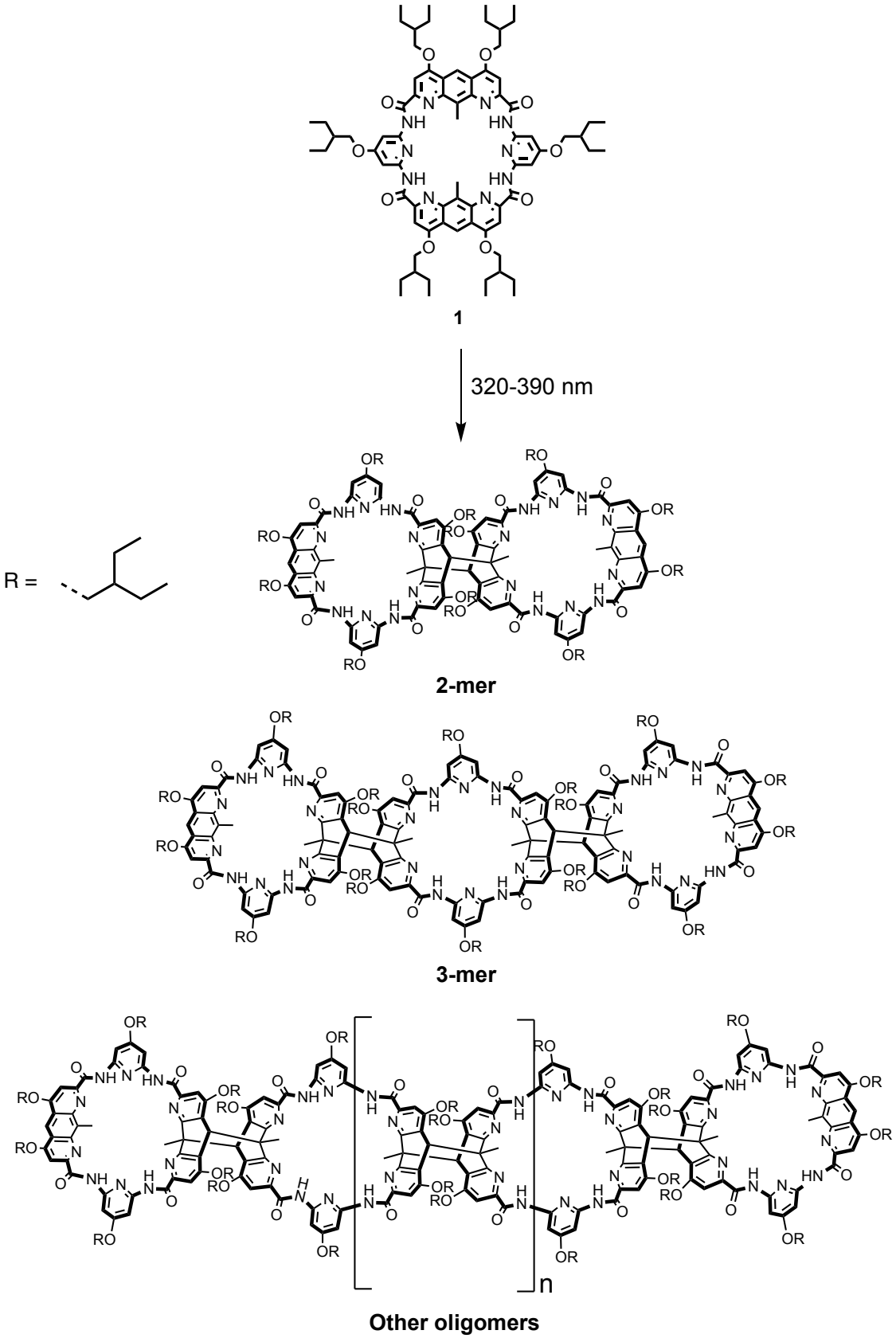

Scheme S4. Macrocycle **1** (15 mg) was dissolved in degassed $CDCl_3$ (0.5 mL) under N_2 atmosphere and then photoirradiated with 320-390 nm light for 3 hours. The changes during the reaction were monitored by ^1H NMR spectra every 30 minutes.

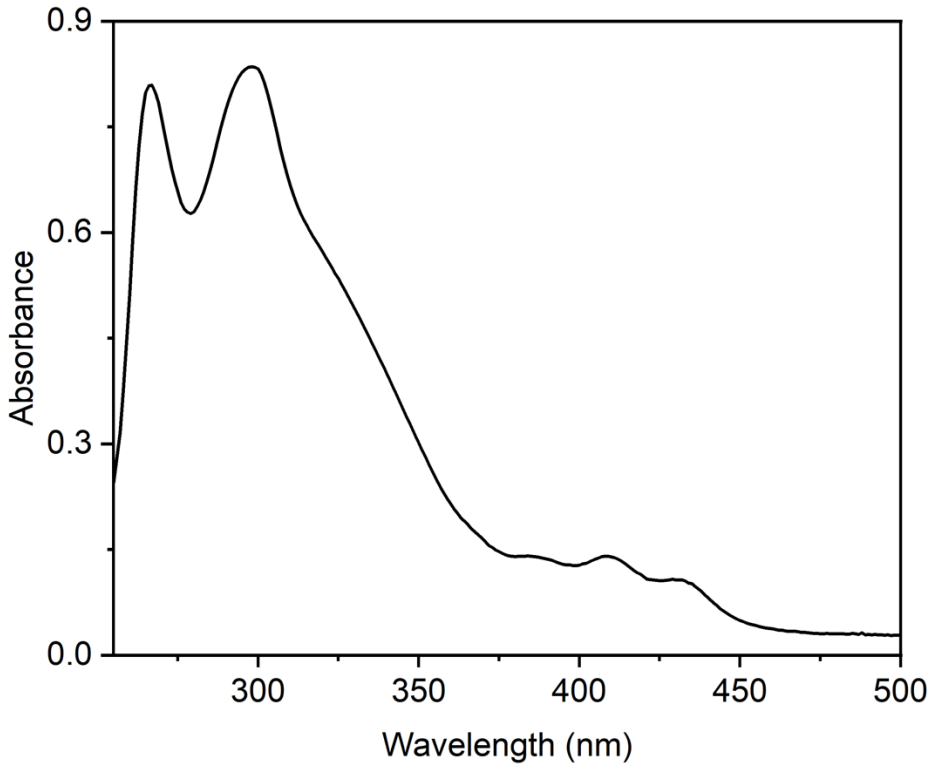

Fig. S5 UV-Vis spectrum of **1** (10 μM) in dichloromethane at 298 K.

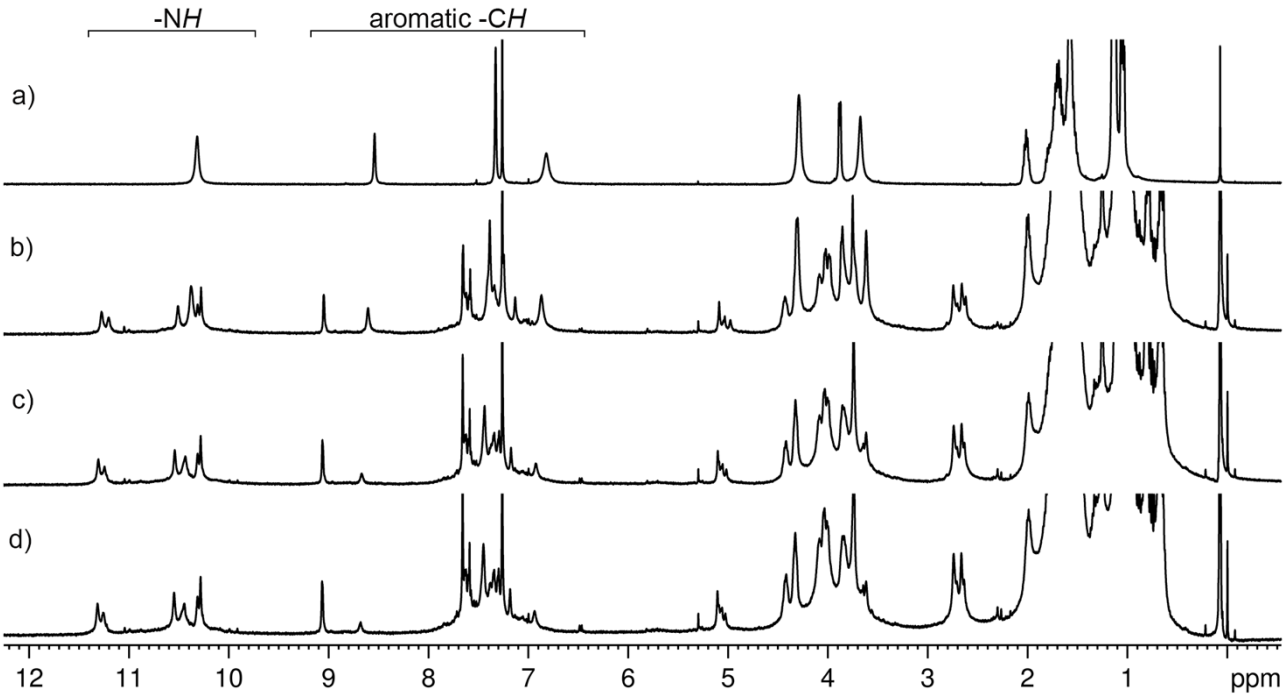

Fig. S6 Stacked representation of 400 MHz ^{1}H-NMR spectra recorded at interval during the photoirradiation of **1** in $CDCl_3$ at 298 K. (a) Macrocycle **1** before irradiation and after (b) 60 min, (c) 120 min and (d) 180 min irradiation.

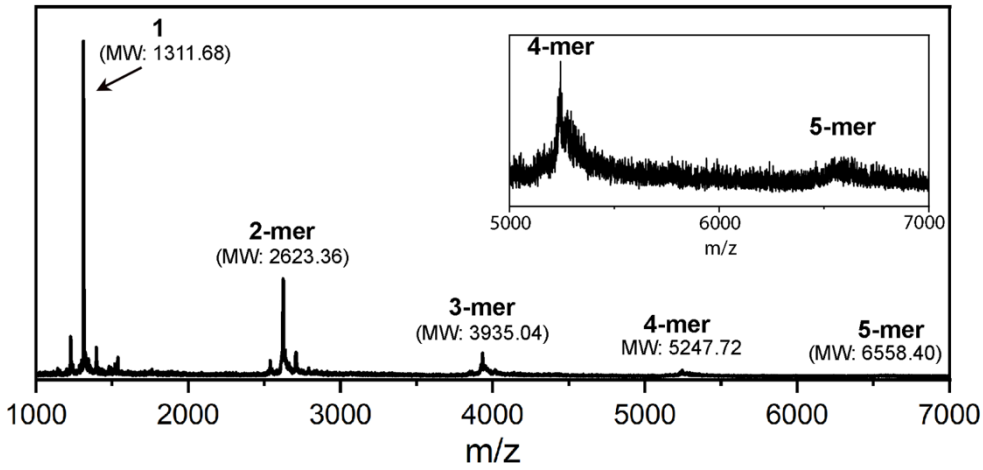

Fig. S7 MALDI-TOF mass spectrum after photoirradiation of **1** for 3 hours. The signal intensity of the higher oligomers is low due to their low ionization.

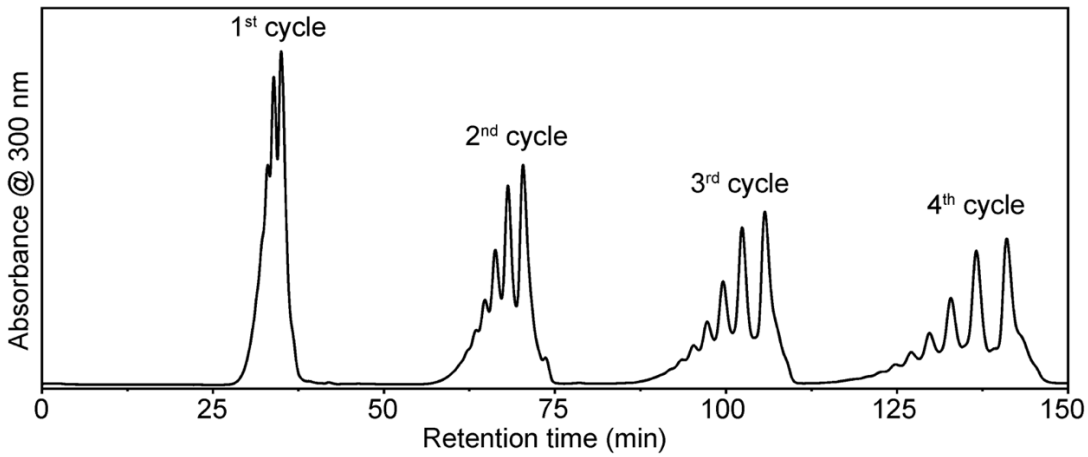

Fig. S8 Recycling GPC profile after photoirradiation of **1**. The oligomers were separated after the fourth cycle.

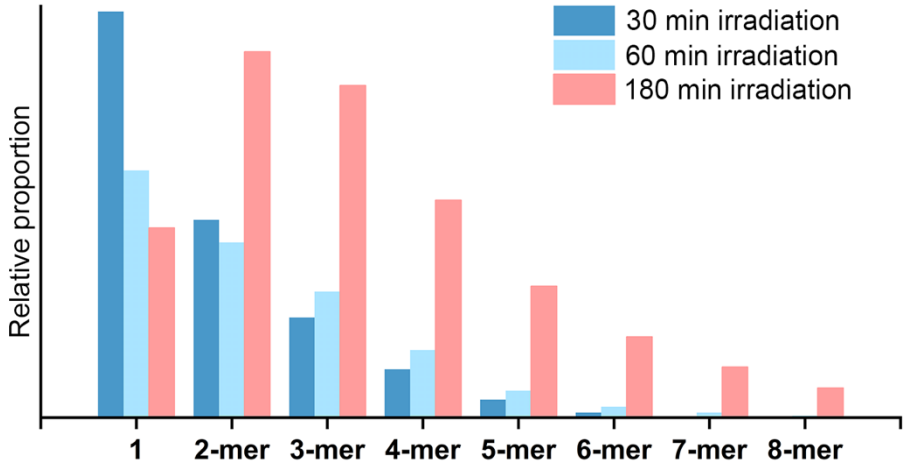

Fig. S9 Bar diagram showing the proportion of different oligomers obtained from the irradiation time.

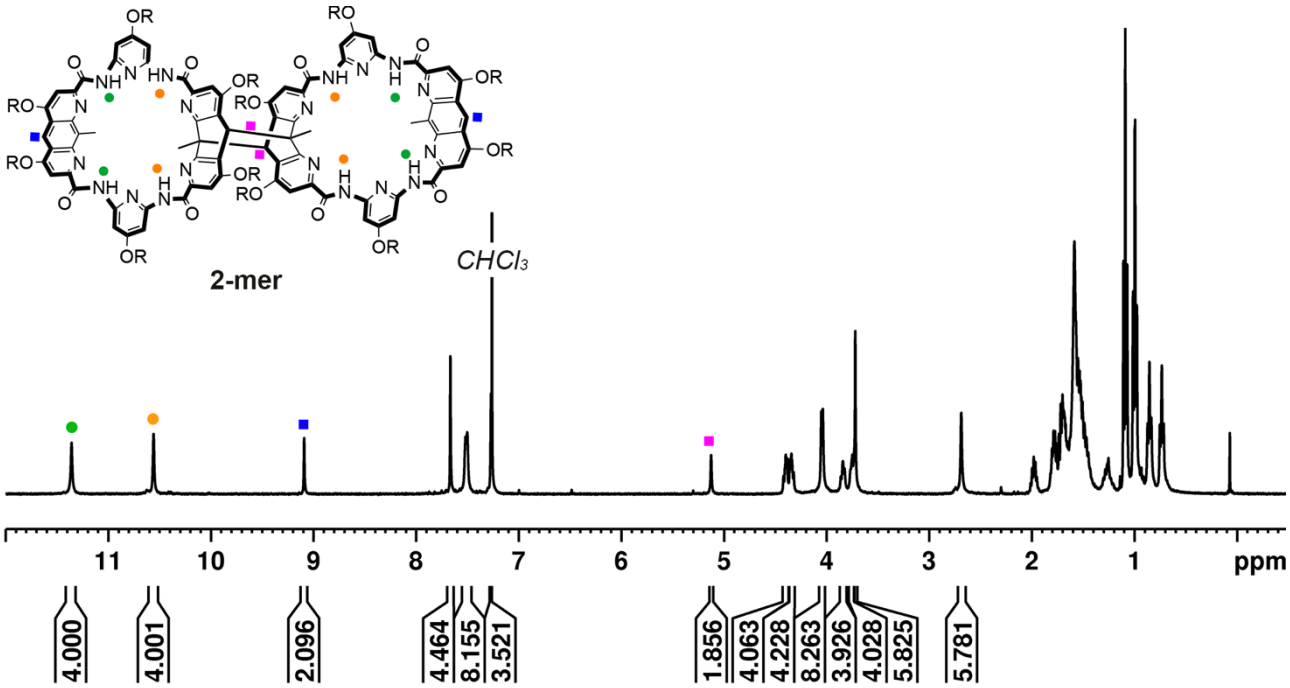

Fig. S10 400 MHz ^{1}H-NMR spectrum of **2-mer** in $CDCl_3$ at 298 K.

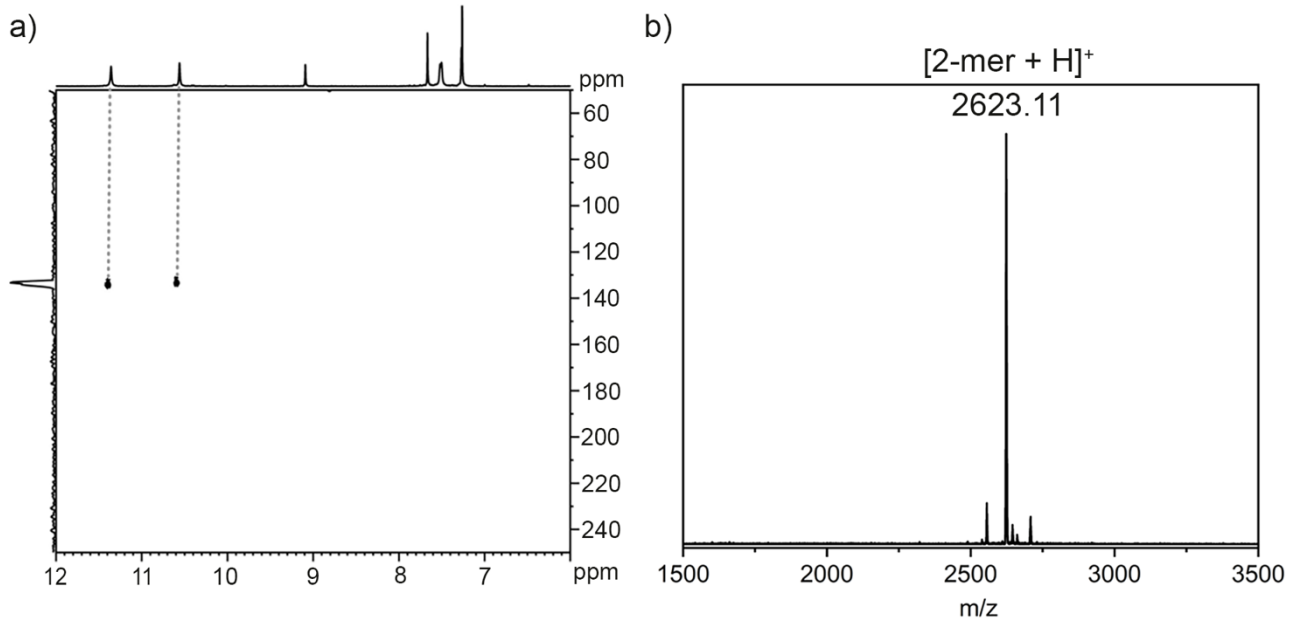

Fig. S11 (a) ^{15}N-^{1}H HSQC spectrum of **2-mer** in $CDCl_3$ at 298 K identifying amide signals. (b) MALDI-TOF mass spectra of **2-mer**. m/z calculated for $C_{152}H_{197}N_{20}O_{20}$ $[M+H]^+$ 2623.50, Found: 2623.11.

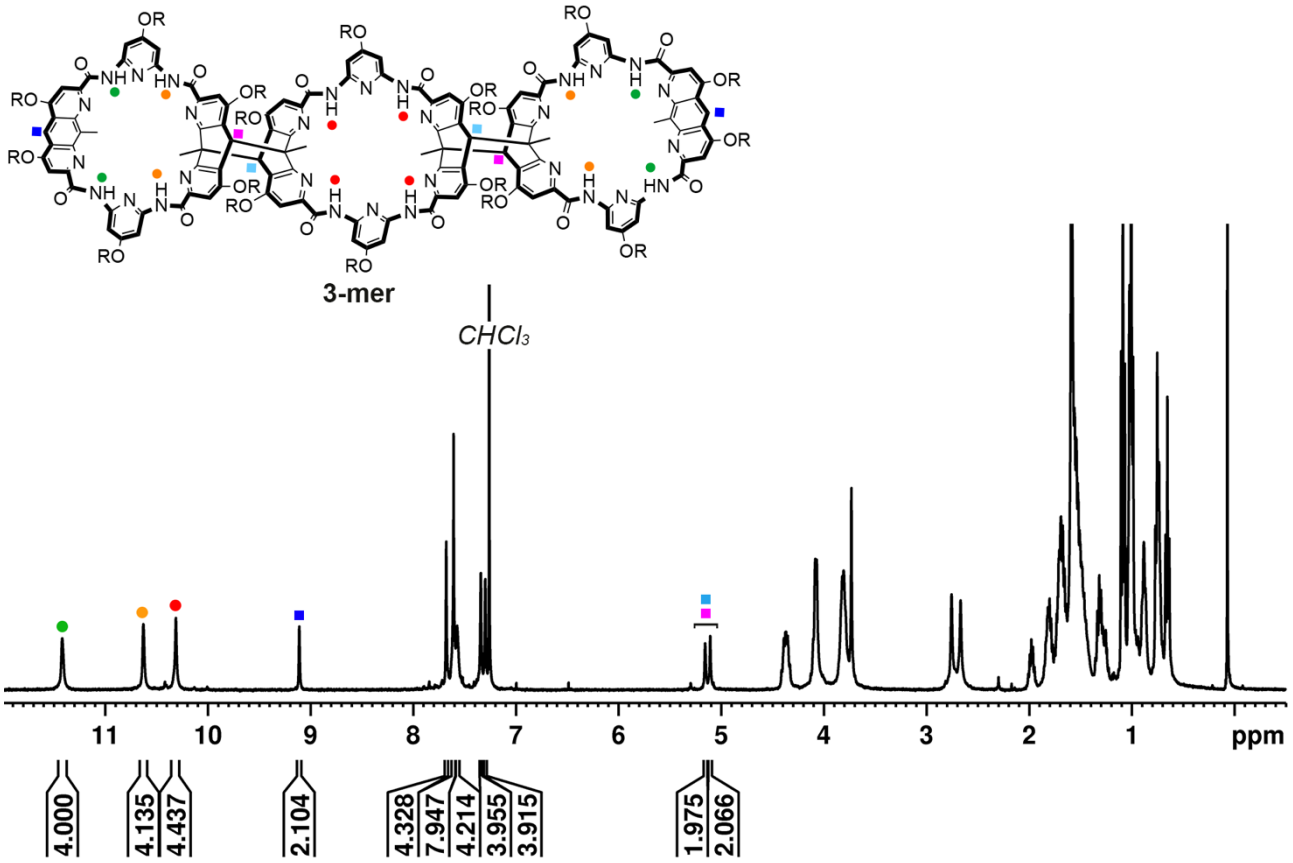

Fig. S12 400 MHz ^{1}H-NMR spectrum of **3-mer** in $CDCl_3$ at 298 K.

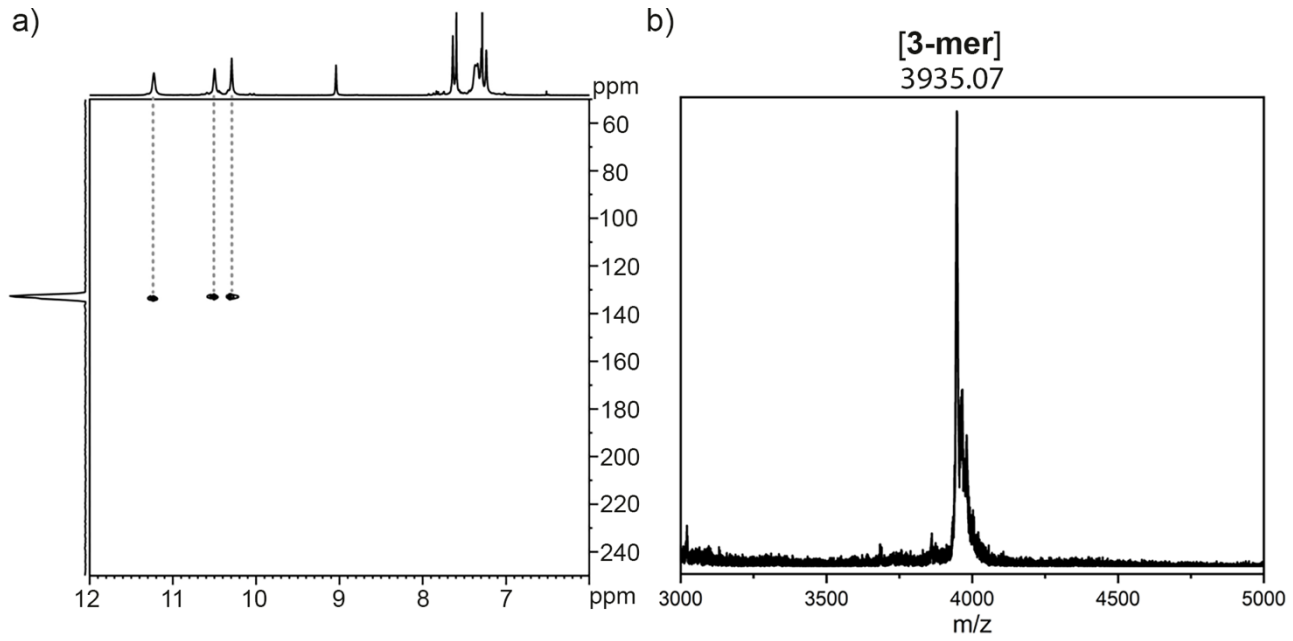

Fig. S13 (a) ^{15}N-^{1}H HSQC spectrum of **3-mer** in $CDCl_3$ at 298 K identifying amide signals. (b) MALDI-TOF mass spectra of **3-mer**. m/z calculated for $C_{228}H_{295}N_{30}O_{30}$ $[M+H]^+$ 3935.25, Found: 3935.07.

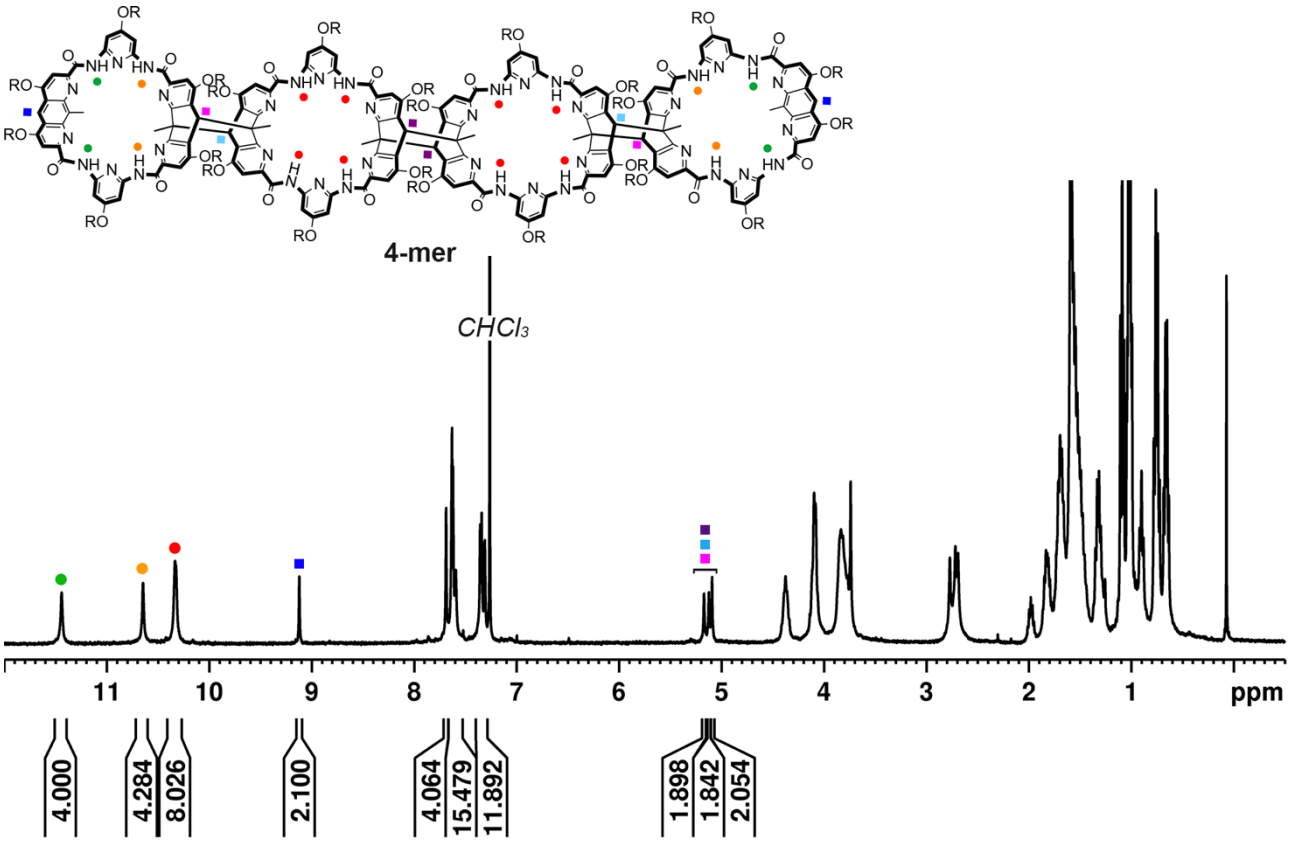

Fig. S14 400 MHz ^{1}H-NMR spectrum of **4-mer** in $CDCl_3$ at 298 K.

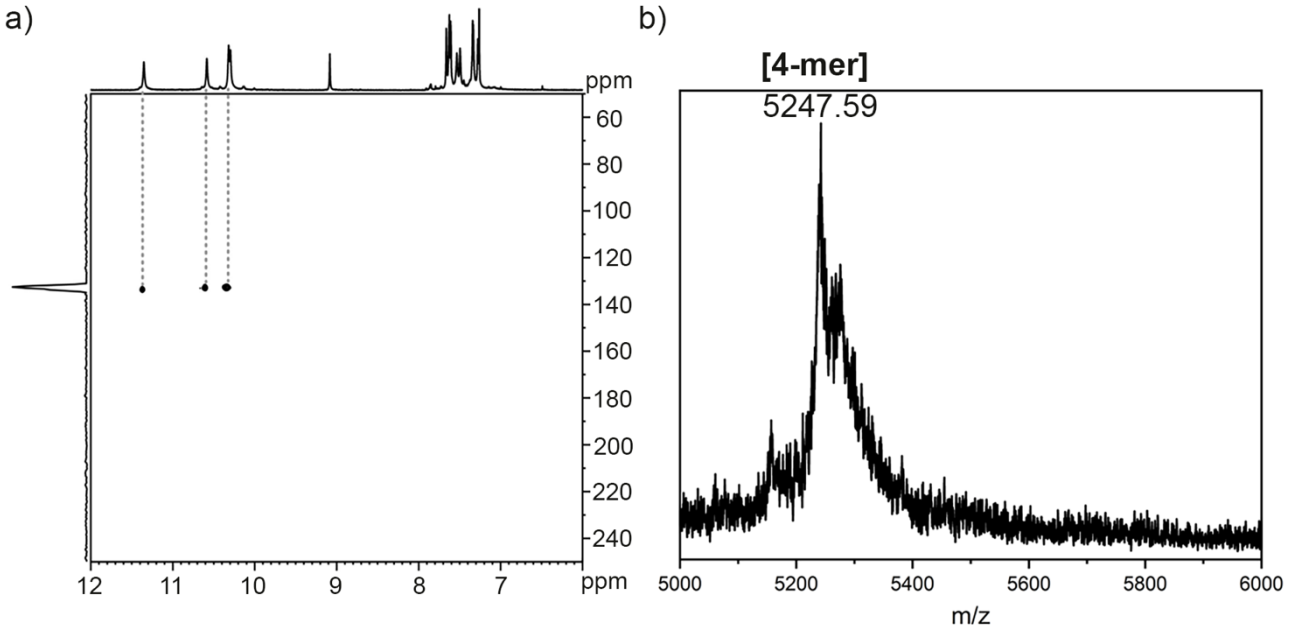

Fig. S15 (a) ^{15}N-^{1}H HSQC spectrum of **4-mer** in $CDCl_3$ at 298 K identifying amide signals. (b) MALDI-TOF mass spectra of **4-mer**. m/z calculated for $C_{304}H_{393}N_{40}O_{40}$ $[M+H]^+$ 5247.01, Found: 5247.59.

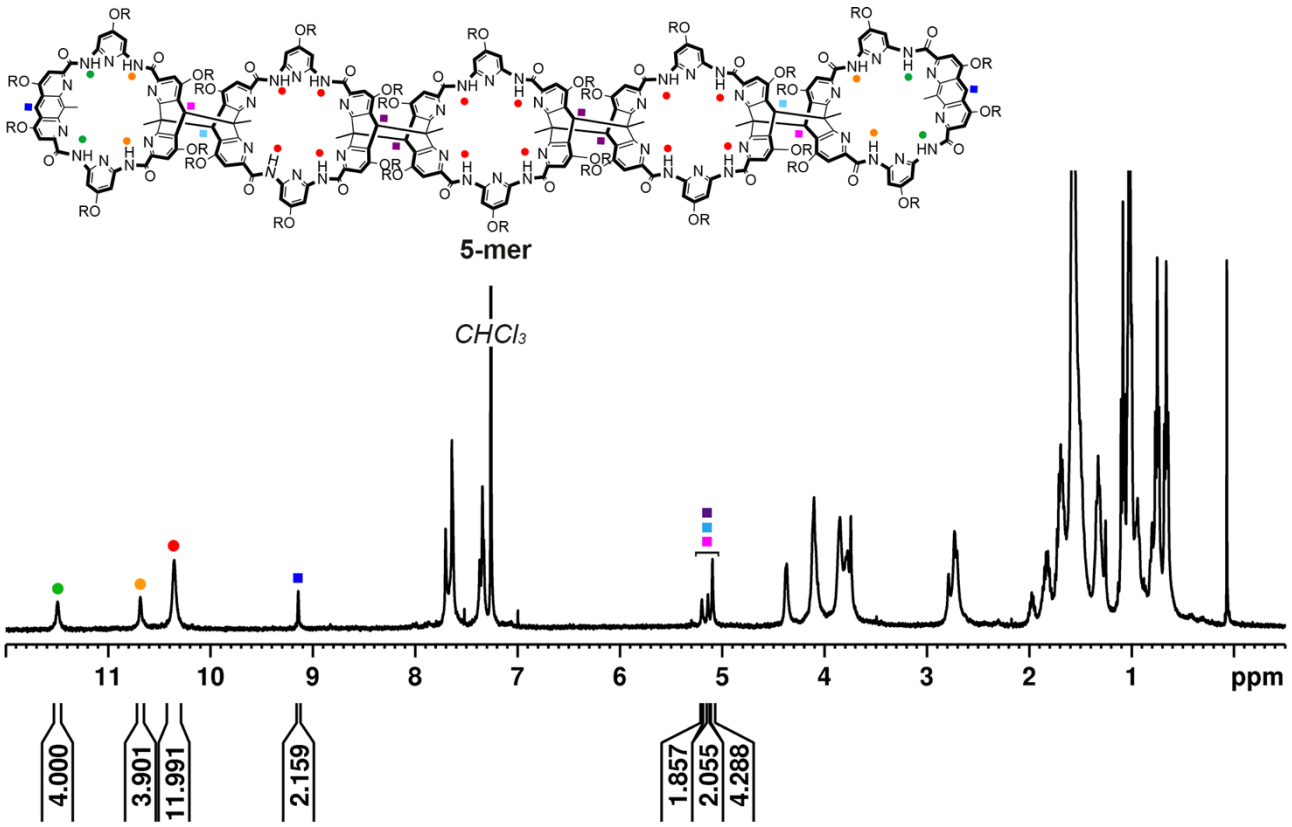

Fig. S16 400 MHz ^{1}H-NMR spectrum of **5-mer** in $CDCl_3$ at 298 K.

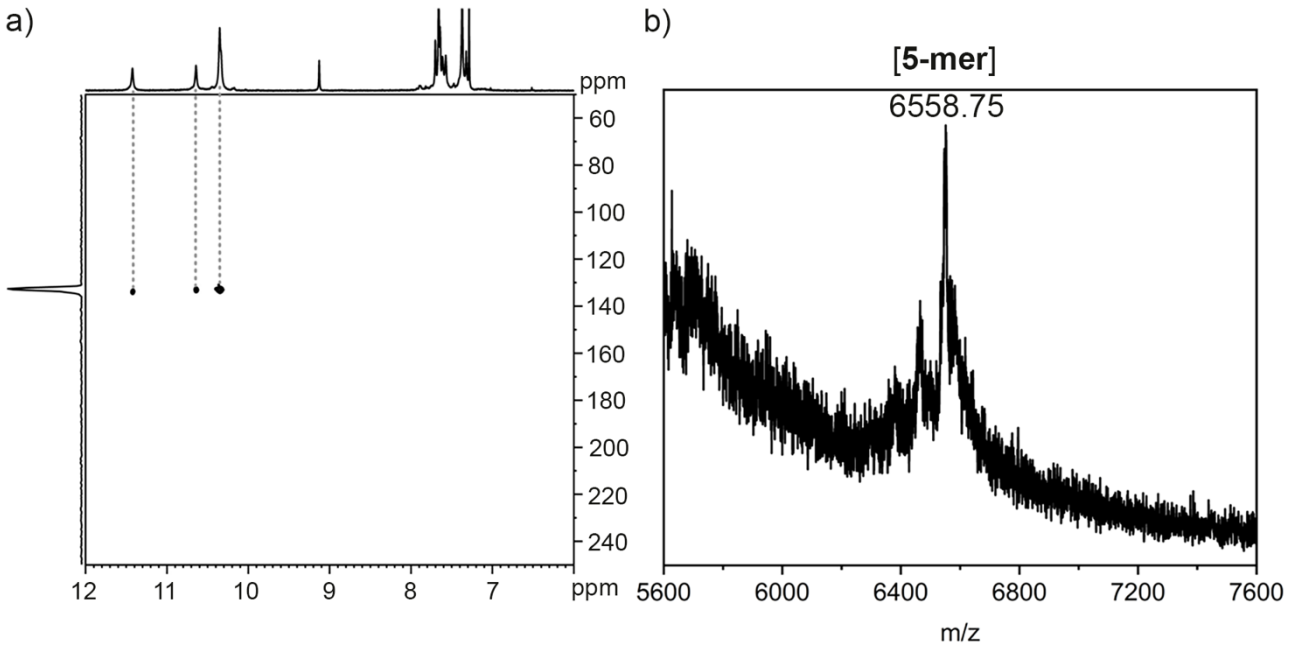

Fig. S17 (a) ^{15}N-^{1}H HSQC spectrum of **5-mer** in $CDCl_3$ at 298 K identifying amide signals. (b) MALDI-TOF mass spectra of **5-mer**. m/z calculated for $C_{380}H_{491}N_{50}O_{50}$ $[M+H]^+$ 6558.75, Found: 6557.72.

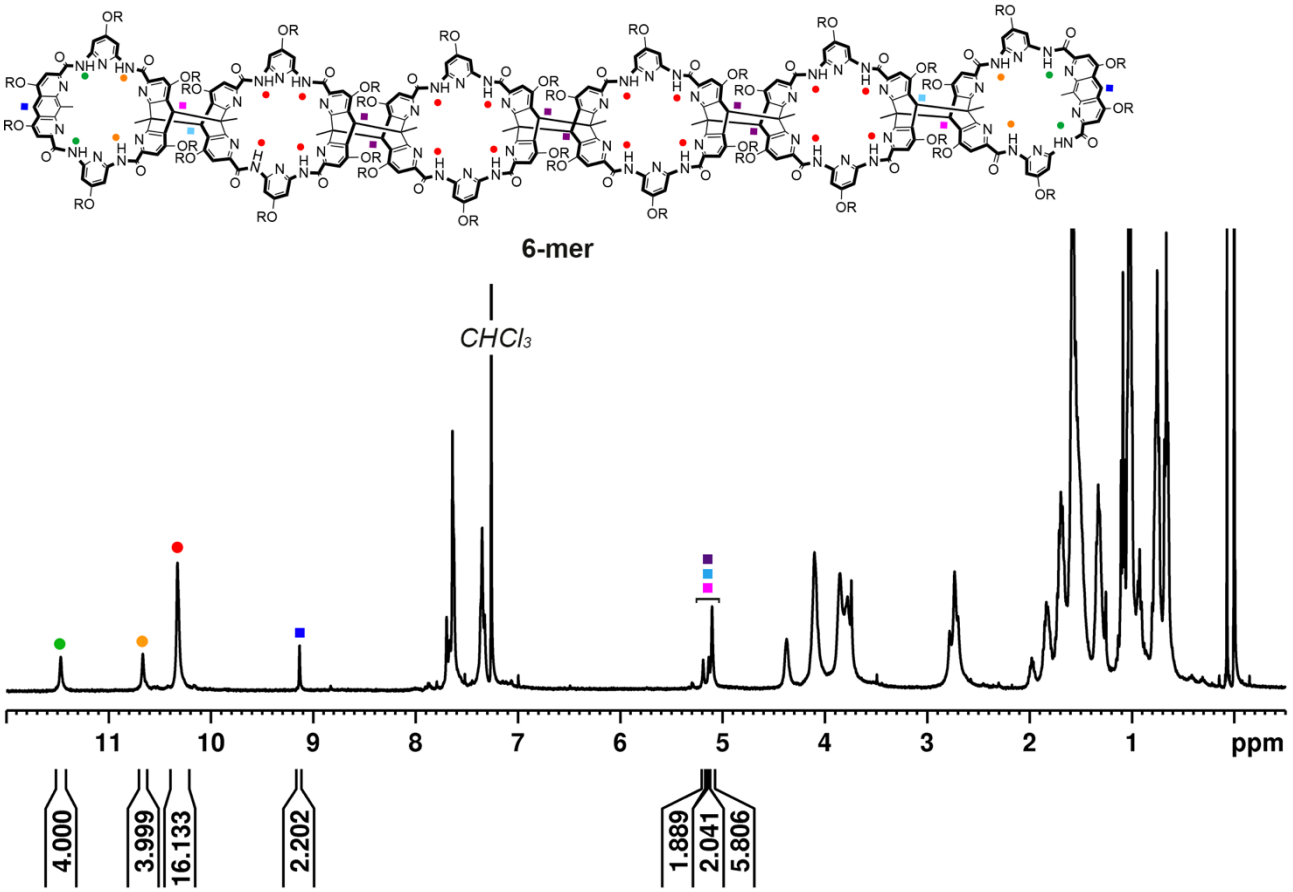

Fig. S18 400 MHz ^{1}H-NMR spectrum of **6-mer** in $CDCl_3$ at 298 K.

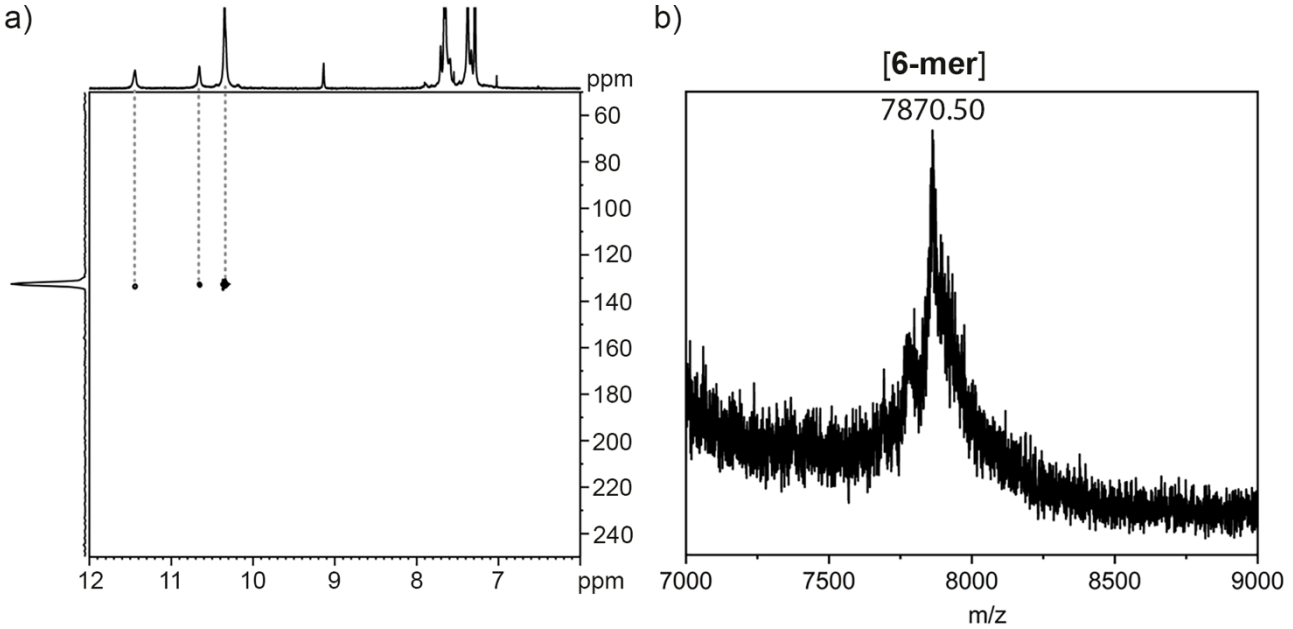

Fig. S19 (a) ^{15}N-^{1}H HSQC spectrum of **6-mer** in $CDCl_3$ at 298 K identifying amide signals. (b) MALDI-TOF mass spectra of **6-mer**. m/z calculated for $C_{456}H_{589}N_{60}O_{60}$ $[M+H]^+$ 7870.50, Found: 7868.26.

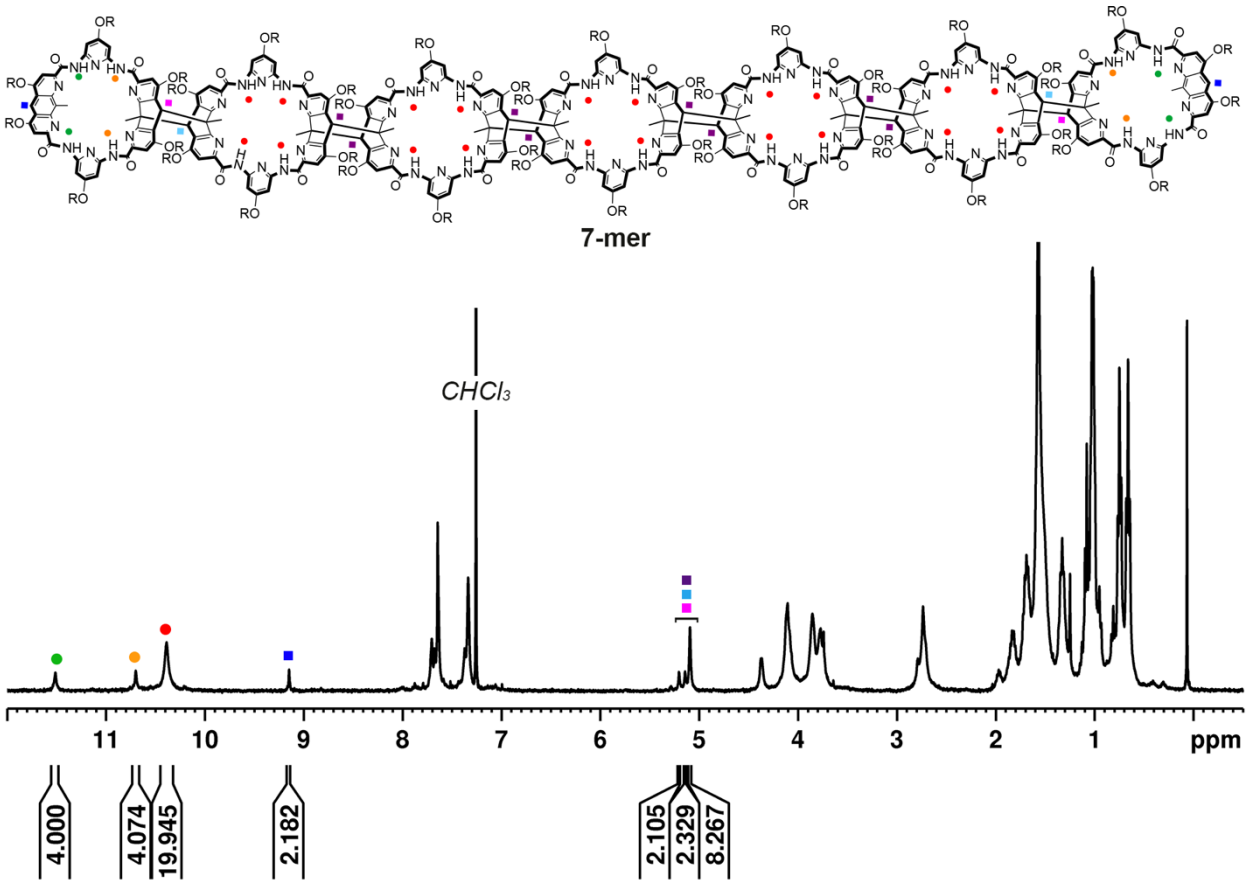

Fig. S20 400 MHz ^{1}H-NMR spectrum of **7-mer** in $CDCl_3$ at 298 K.

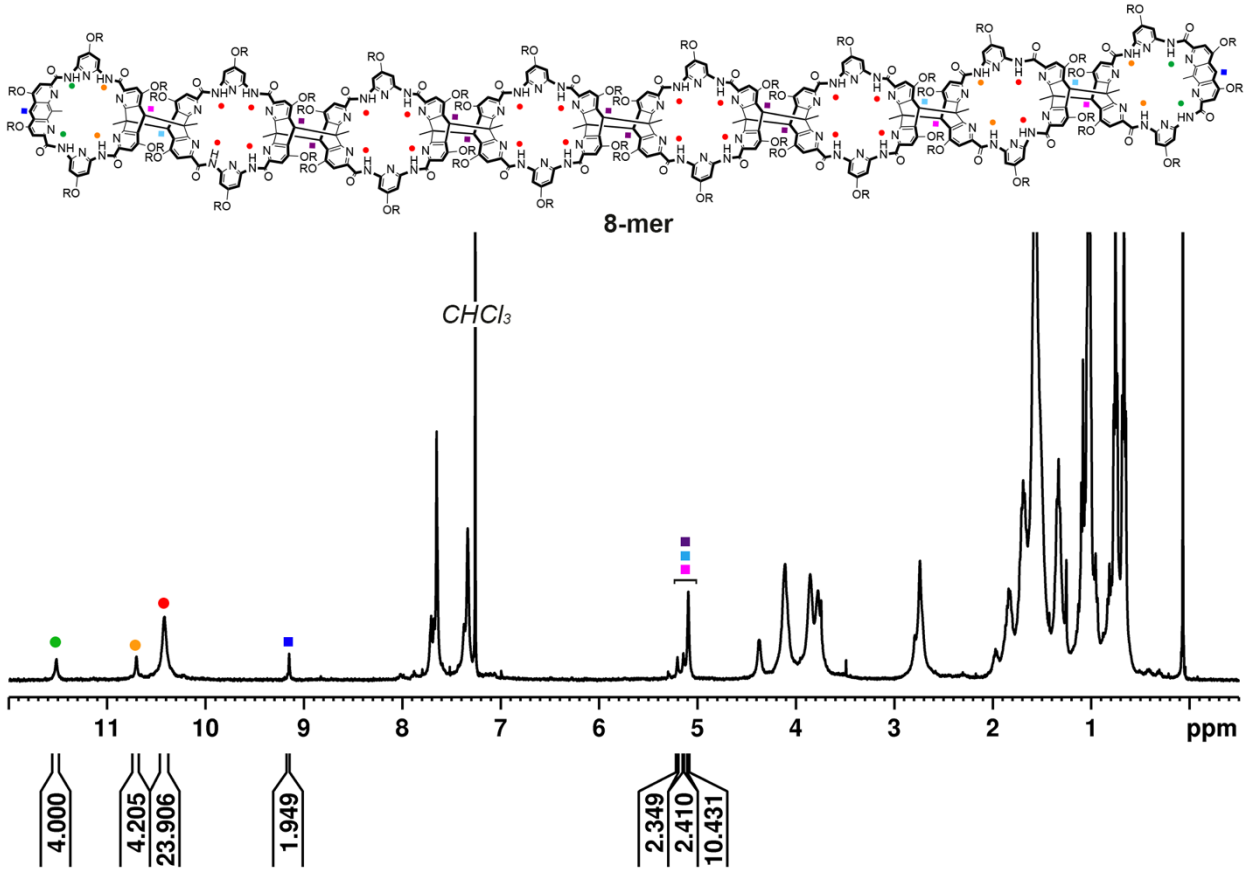

Fig. S21 400 MHz ^{1}H-NMR spectrum of **8-mer** in $CDCl_3$ at 298 K.

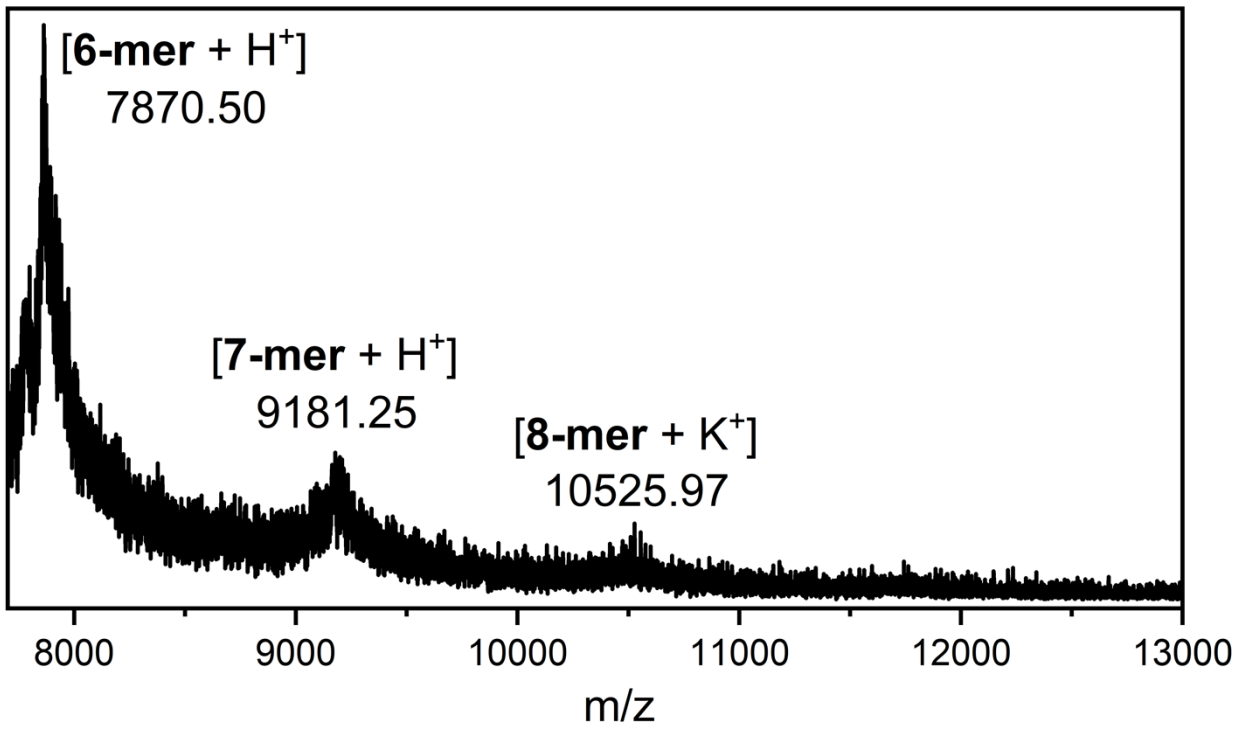

Fig. S22 MALDI-TOF mass spectra of **8-mer** where peaks for **7-mer** and **6-mer** were also observed due to the degradation under the experimental condition.

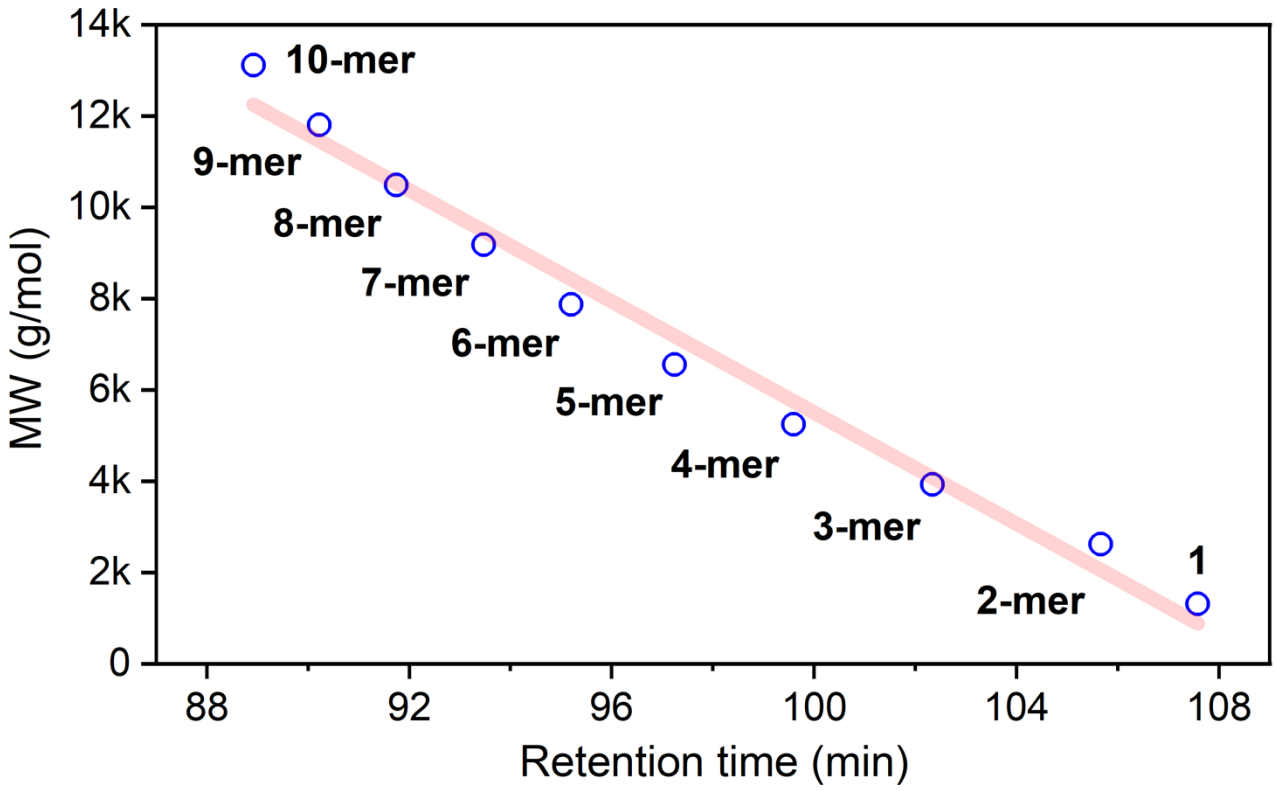

Fig. S23 Variation of theoretical molecular weight (MW) of the oligomers with retention time. A linear correlation indicates the rigid nature of the oligomers. The retention time was considered after the third cycle in the recycling GPC for clarity.

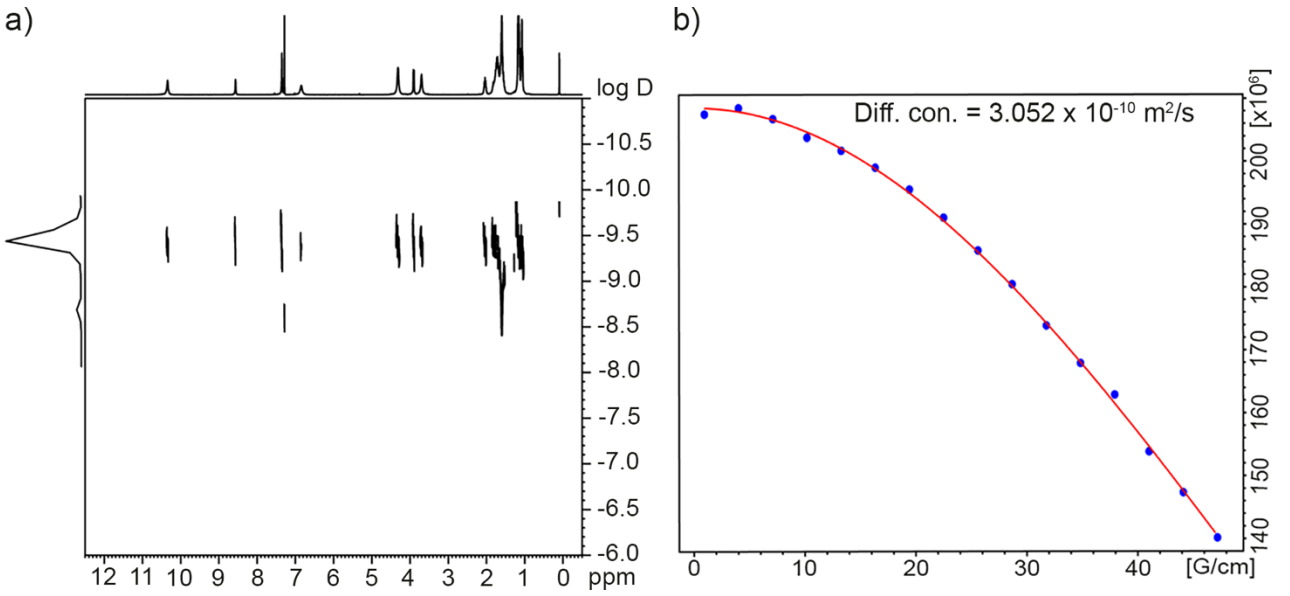

Fig. S24 (a) ^{1}H DOSY spectrum of **1** in $CDCl_3$ at 298 K. (b) The diffusion coefficient was calculated after processing the experimental DOSY spectrum with the T1/T2 software. Blue points represent peak intensities as a function of increasing gradient strength, and the red line represents the regression fit.

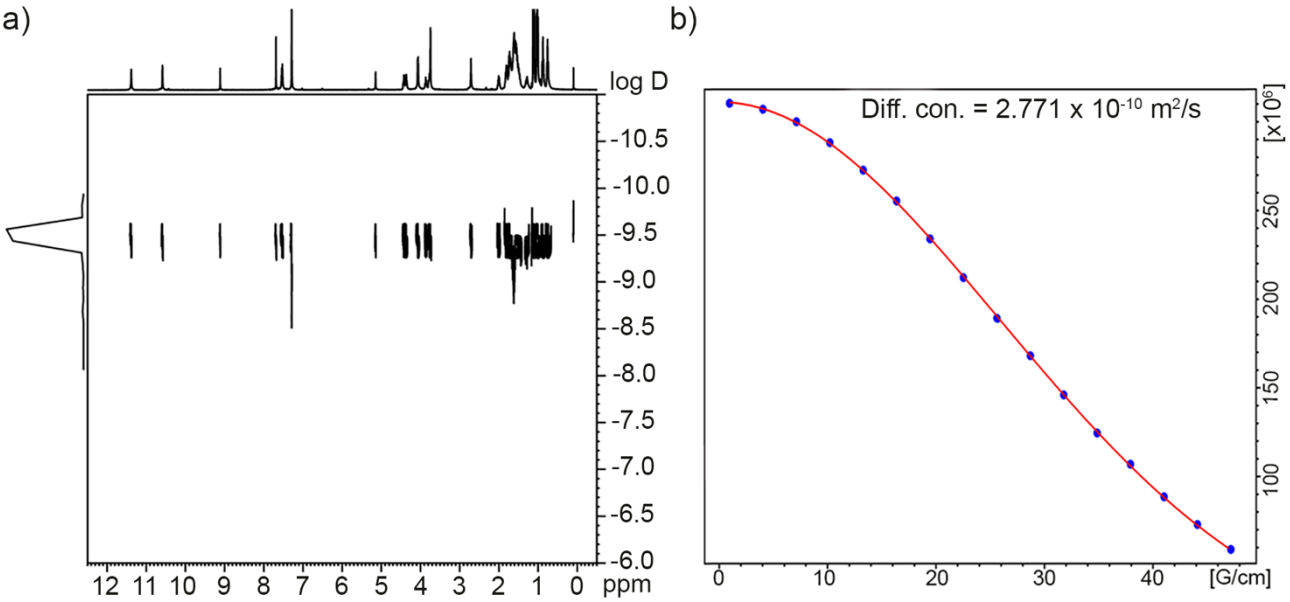

Fig. S25 (a) ^{1}H DOSY spectrum of **2-mer** in $CDCl_3$ at 298 K. (b) The diffusion coefficient was calculated after processing the experimental DOSY spectrum with the T1/T2 software. Blue points represent peak intensities as a function of increasing gradient strength, and the red line represents the regression fit.

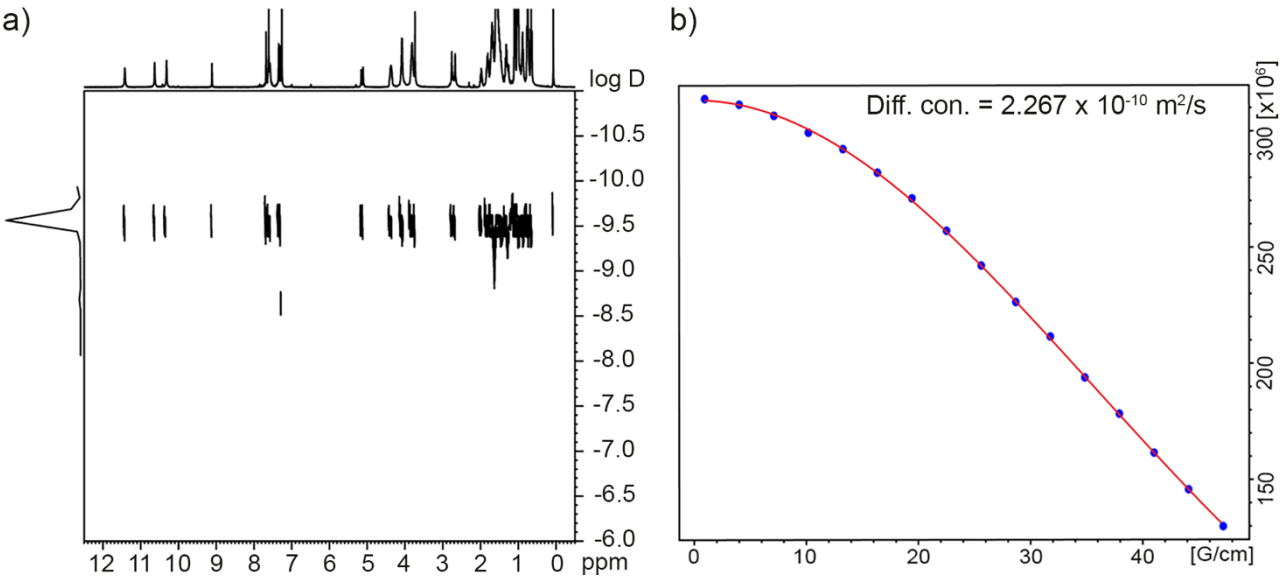

Fig. S26 (a) ^{1}H DOSY spectrum of **3-mer** in $CDCl_3$ at 298 K. (b) The diffusion coefficient was calculated after processing the experimental DOSY spectrum with the T1/T2 software. Blue points represent peak intensities as a function of increasing gradient strength, and the red line represents the regression fit.

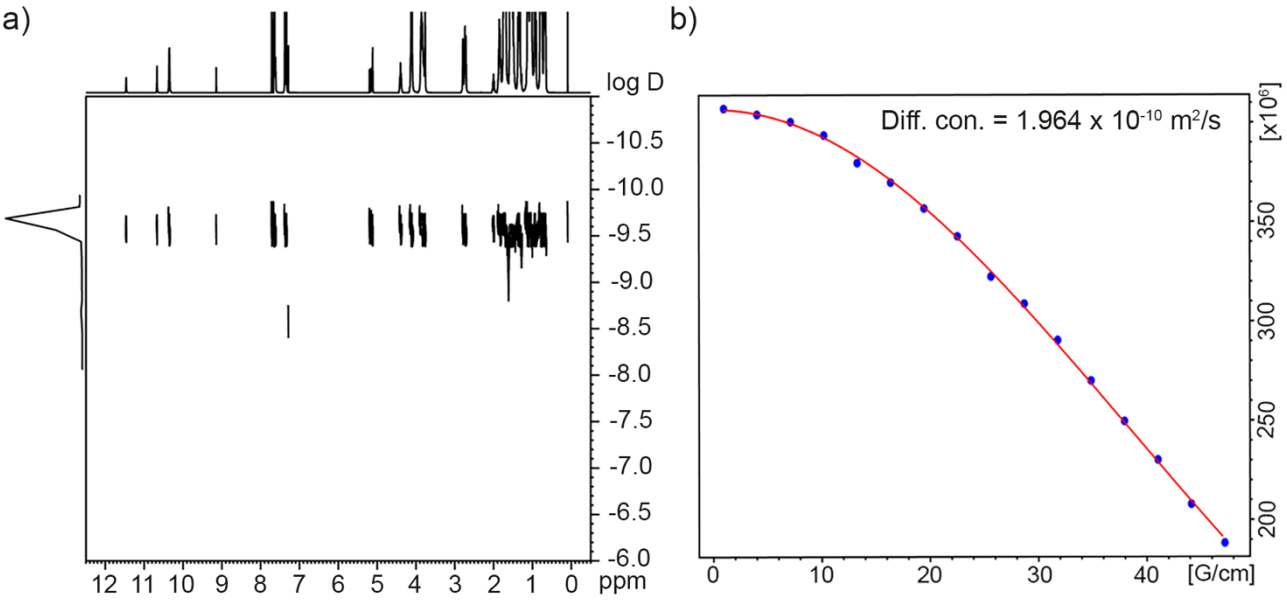

Fig. S27 (a) ^{1}H DOSY spectrum of **4-mer** in $CDCl_3$ at 298 K. (b) The diffusion coefficient was calculated after processing the experimental DOSY spectrum with the T1/T2 software. Blue points represent peak intensities as a function of increasing gradient strength, and the red line represents the regression fit.

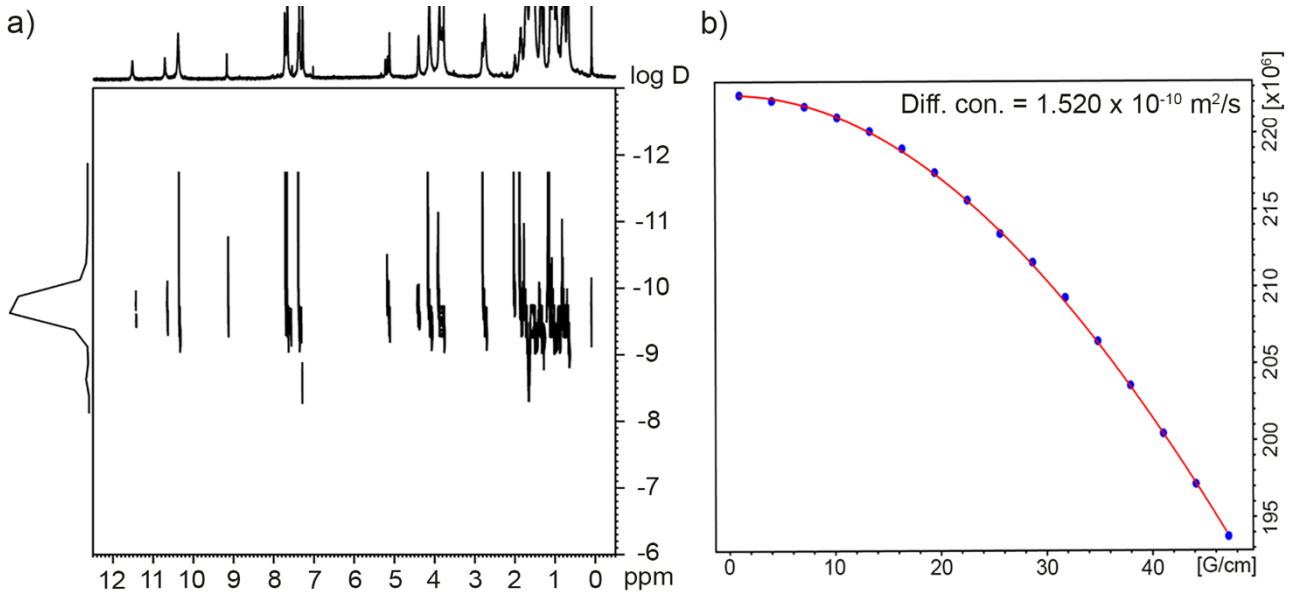

Fig. S28 (a) ^{1}H DOSY spectrum of **5-mer** in $CDCl_3$ at 298 K. (b) The diffusion coefficient was calculated after processing the experimental DOSY spectrum with the T1/T2 software. Blue points represent peak intensities as a function of increasing gradient strength, and the red line represents the regression fit.

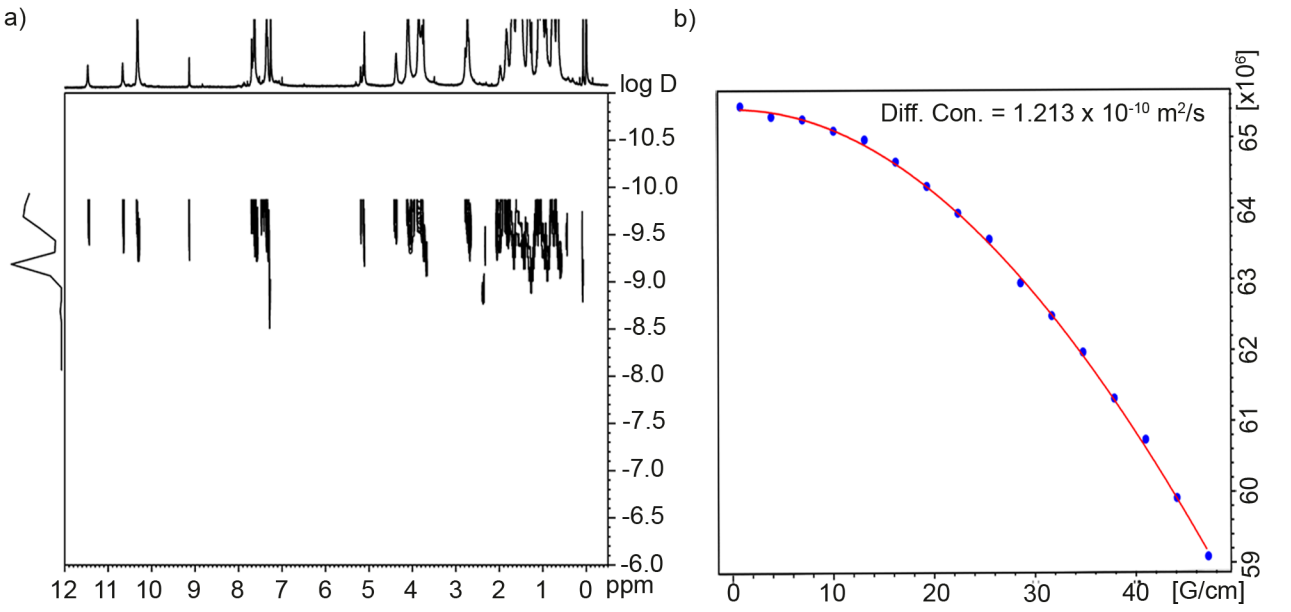

Fig. S29 (a) ^{1}H DOSY spectrum of **6-mer** in $CDCl_3$ at 298 K. (b) The diffusion coefficient was calculated after processing the experimental DOSY spectrum with the T1/T2 software. Blue points represent peak intensities as a function of increasing gradient strength, and the red line represents the regression fit.

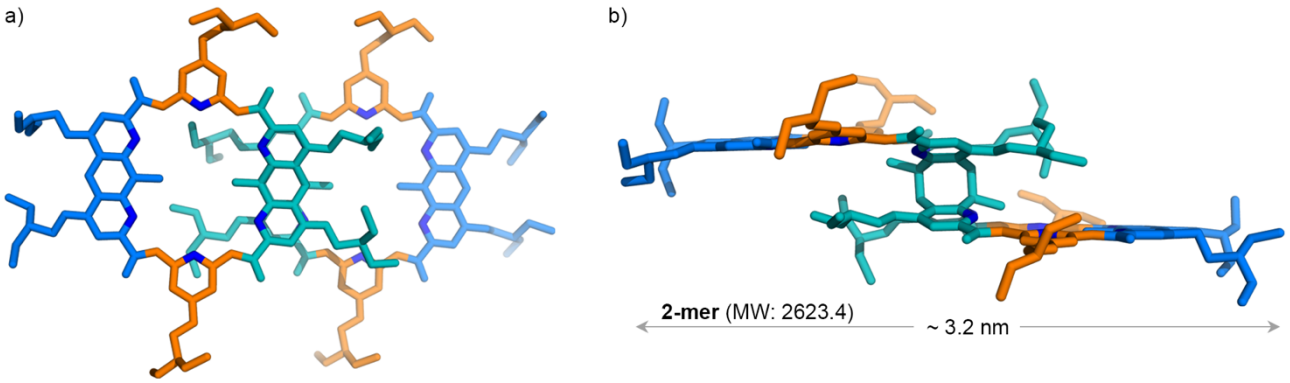

Fig. S30 (a) and (b) Top and side view of the energy-minimized molecular model of **2-mer**, respectively, using the Merck Molecular Force Field static (MMFFs) shown in tube representation. Hydrogen atoms are omitted for clarity.

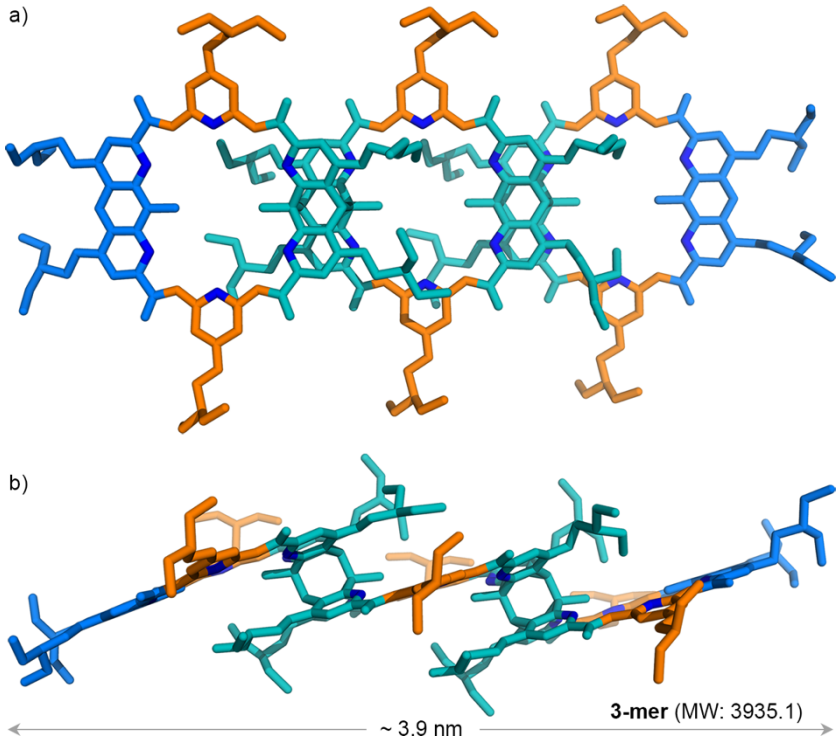

Fig. S31 (a) and (b) Top and side view of the energy-minimized molecular model of **3-mer**, respectively, using the Merck Molecular Force Field static (MMFFs) shown in tube representation. Hydrogen atoms are omitted for clarity.

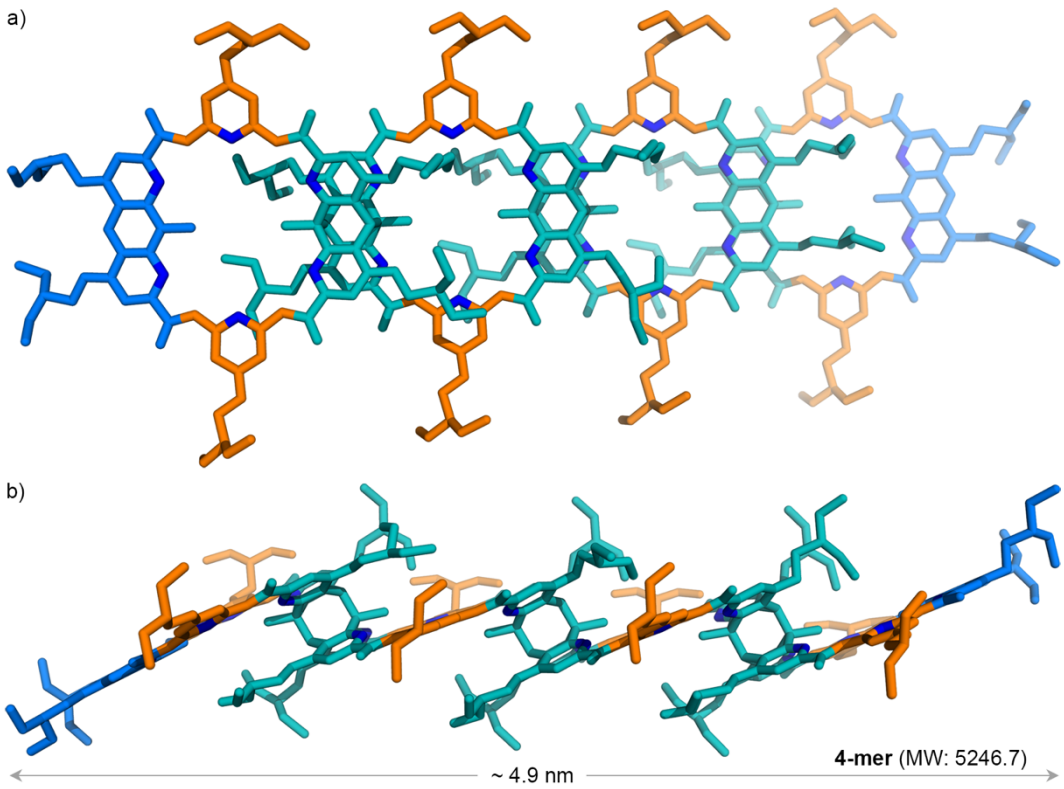

Fig. S32 (a) and (b) Top and side view of the energy-minimized molecular model of **4-mer**, respectively, using the Merck Molecular Force Field static (MMFFs) shown in tube representation. Hydrogen atoms are omitted for clarity.

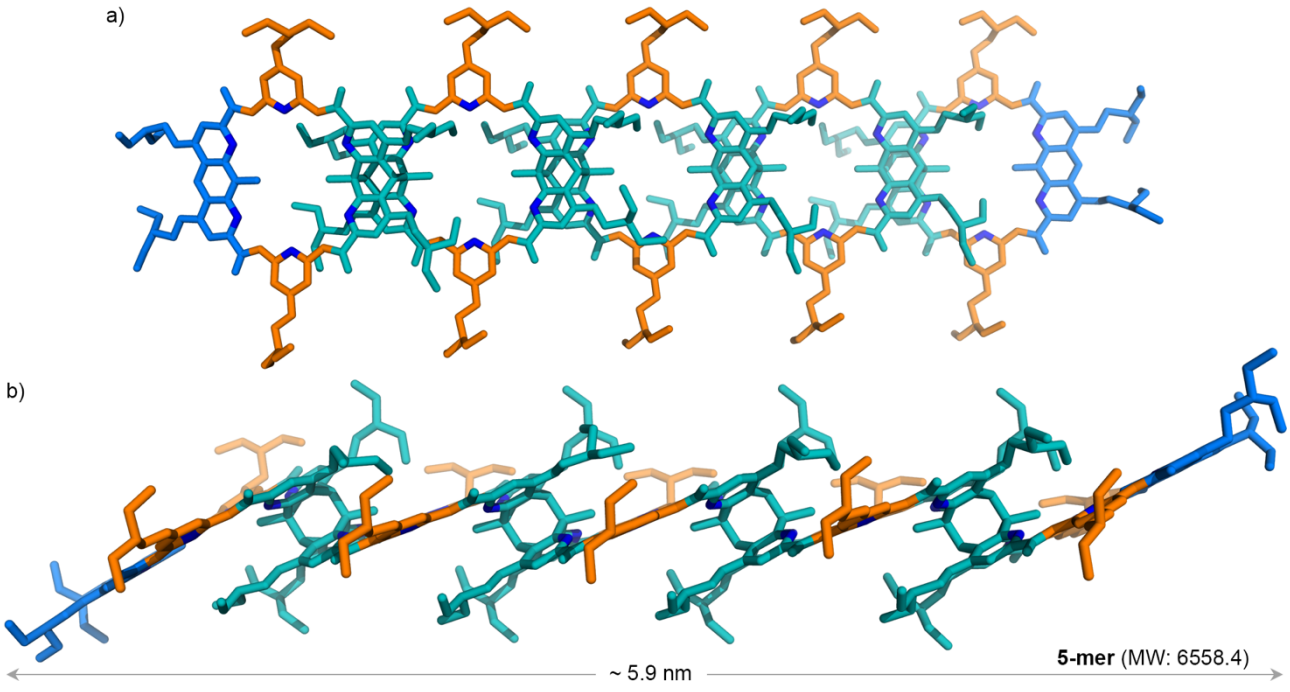

Fig. S33 (a) and (b) Top and side view of the energy-minimized molecular model of **5-mer**, respectively, using the Merck Molecular Force Field static (MMFFs) shown in tube representation. Hydrogen atoms are omitted for clarity.

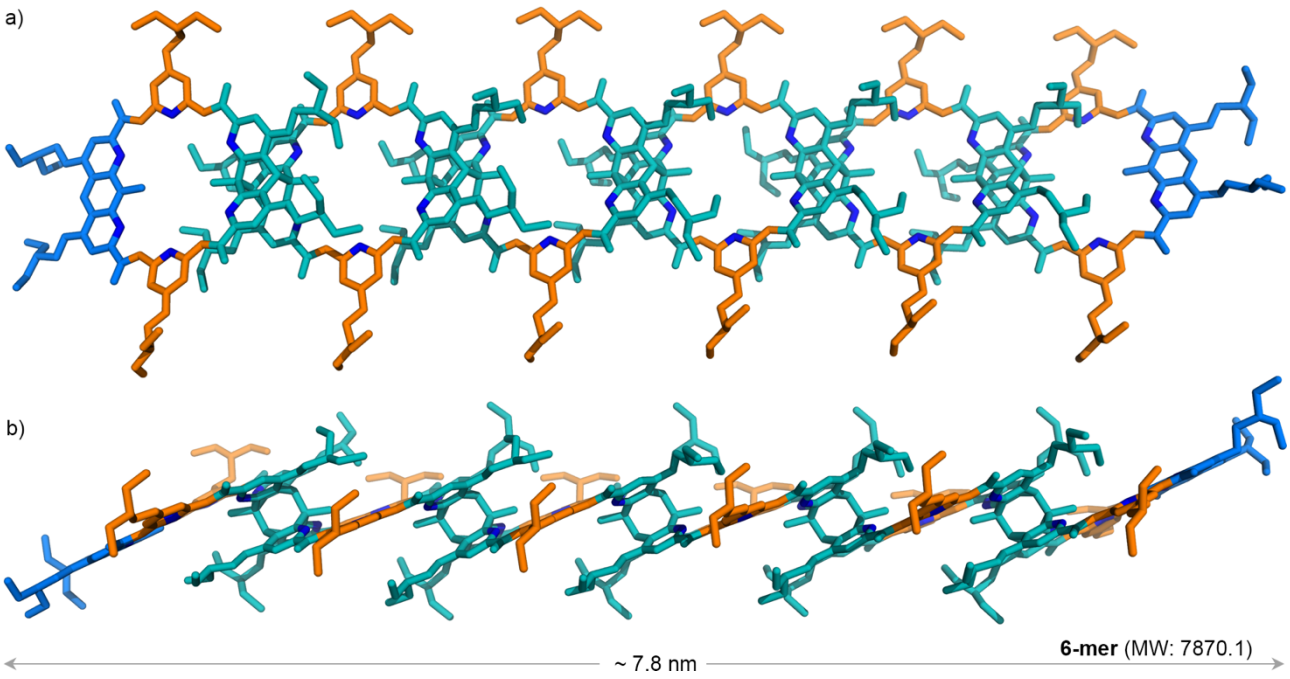

Fig. S34 (a) and (b) Top and side view of the energy-minimized molecular model of **6-mer**, respectively, using the Merck Molecular Force Field static (MMFFs) shown in tube representation. Hydrogen atoms are omitted for clarity.

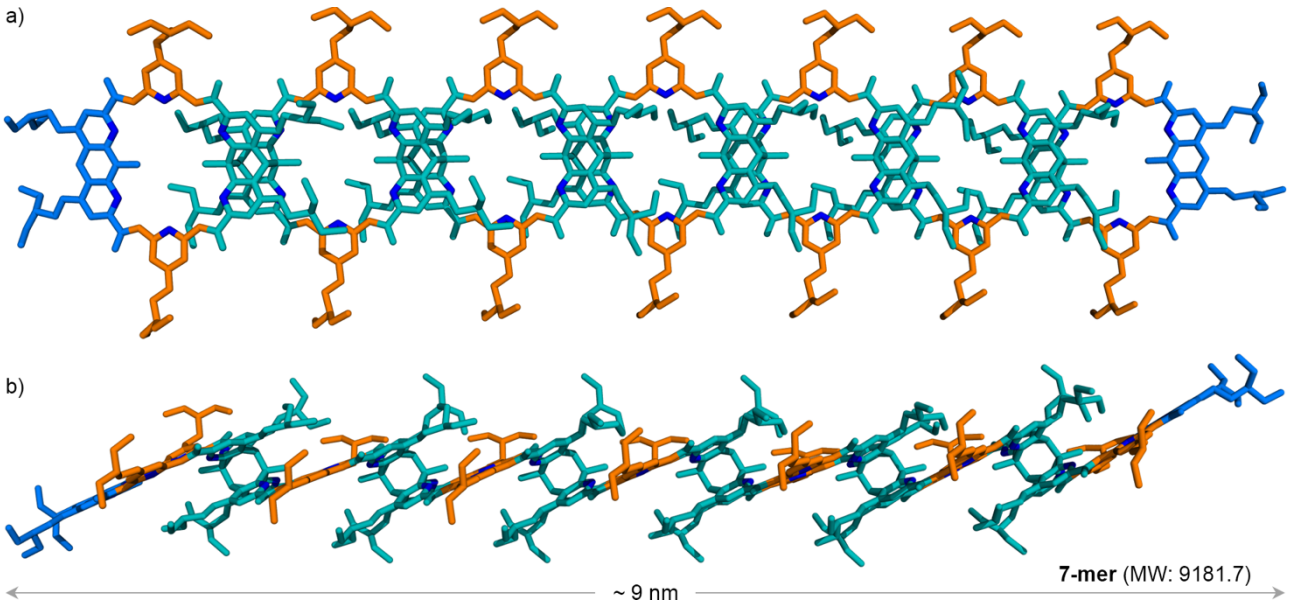

Fig. S35 (a) and (b) Top and side view of the energy-minimized molecular model of **7-mer**, respectively, using the Merck Molecular Force Field static (MMFFs) shown in tube representation. Hydrogen atoms are omitted for clarity.

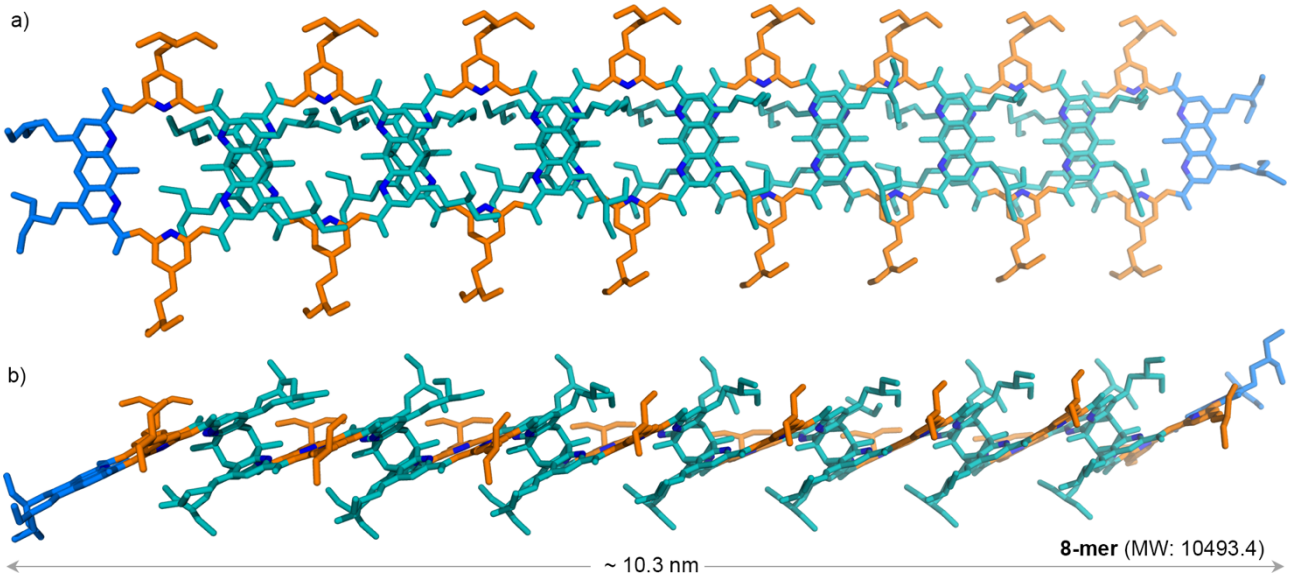

Fig. S36 (a) and (b) Top and side view of the energy-minimized molecular model of **8-mer**, respectively, using the Merck Molecular Force Field static (MMFFs) shown in tube representation. Hydrogen atoms are omitted for clarity.

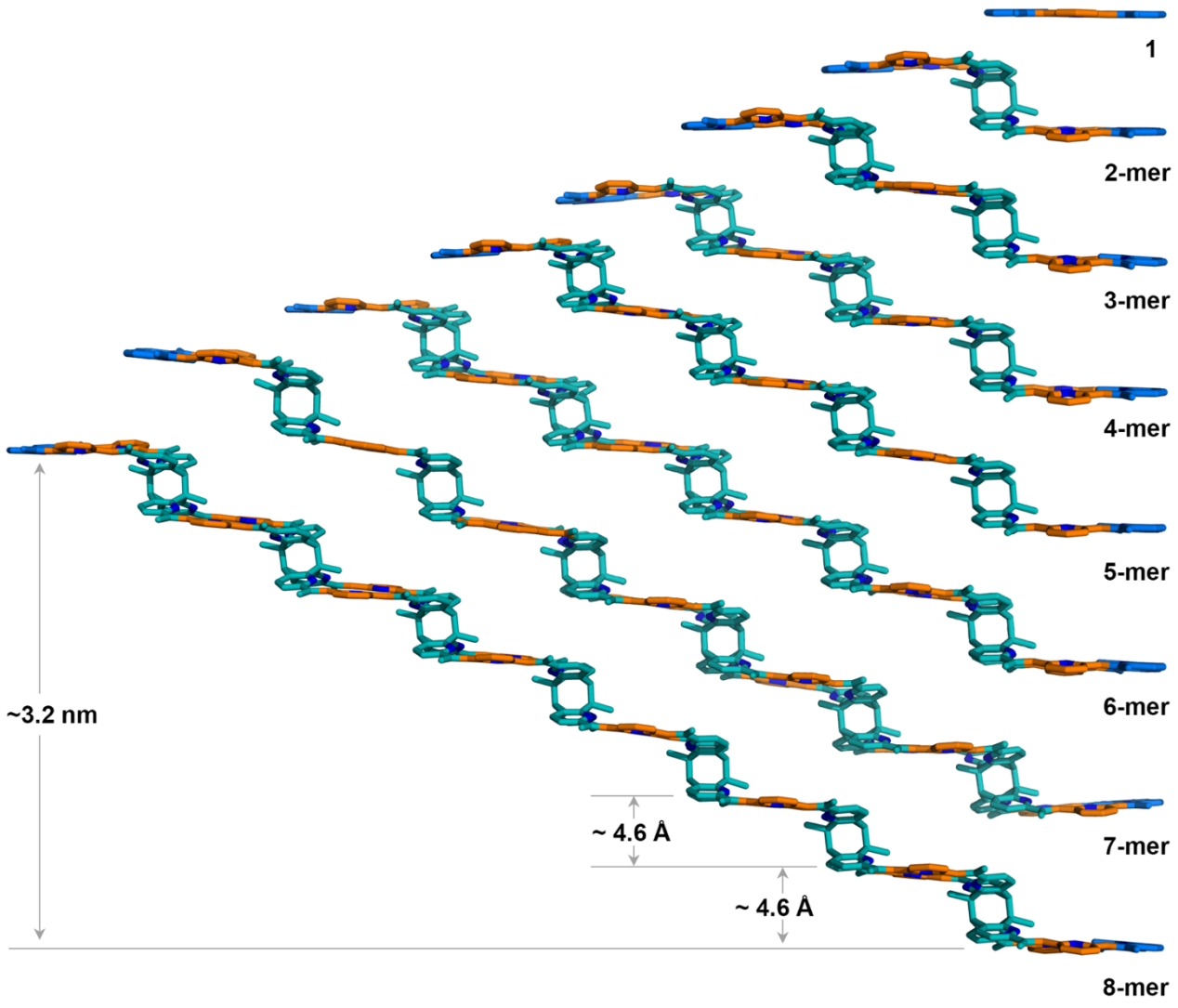

Fig. S37 Energy-minimized molecular model of oligomers showing stairs-like structures with an average step size of 4.6 Å. Side chains and hydrogen atoms are omitted for clarity.

Thermal reversibility experiment: To check thermal reversibility, **4-mer** (5 mg) was dissolved in tetrachloroethane and then subjected to heating at 393 K. Changes were monitored through ^{1}H-NMR at different time intervals. Eventually after heating for 60 hours, the **4-mer** completely converted back to the monomer **1**.

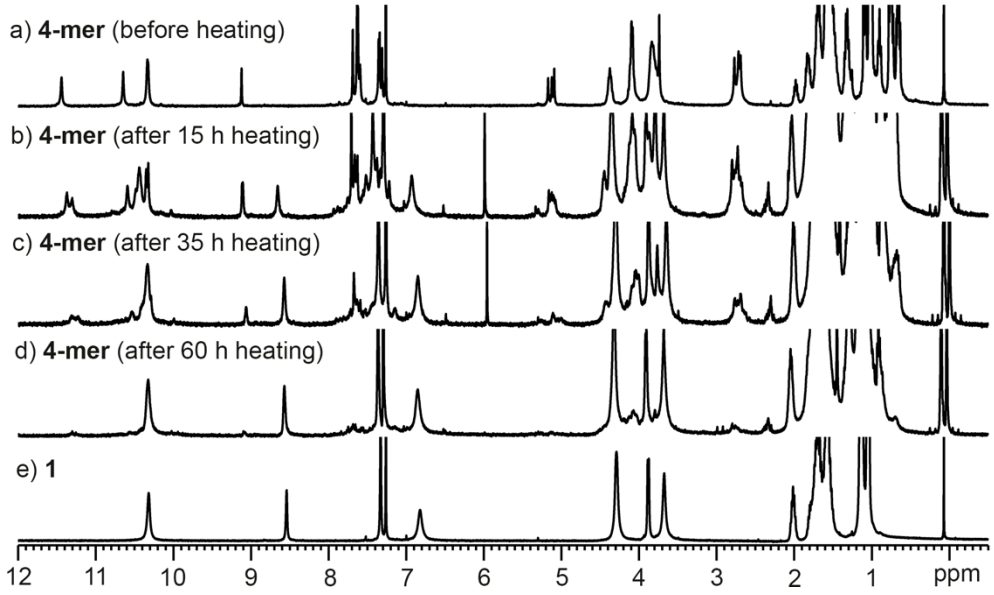

Fig. S38 Stacked 400 MHz ^{1}H-NMR plot for reversibility test of **4-mer**; (a) before heating, (b) after 15 hours heating, (c) After 35 hours heating, and (d) after 60 hours heating at 393 K in tetrachloroethane. (e) The ^{1}H-NMR of **1** is given as a reference. The thermally converted product matches with the ^{1}H-NMR of **1**. The ^{1}H-NMR spectra were recorded in $CDCl_3$ at 298 K.

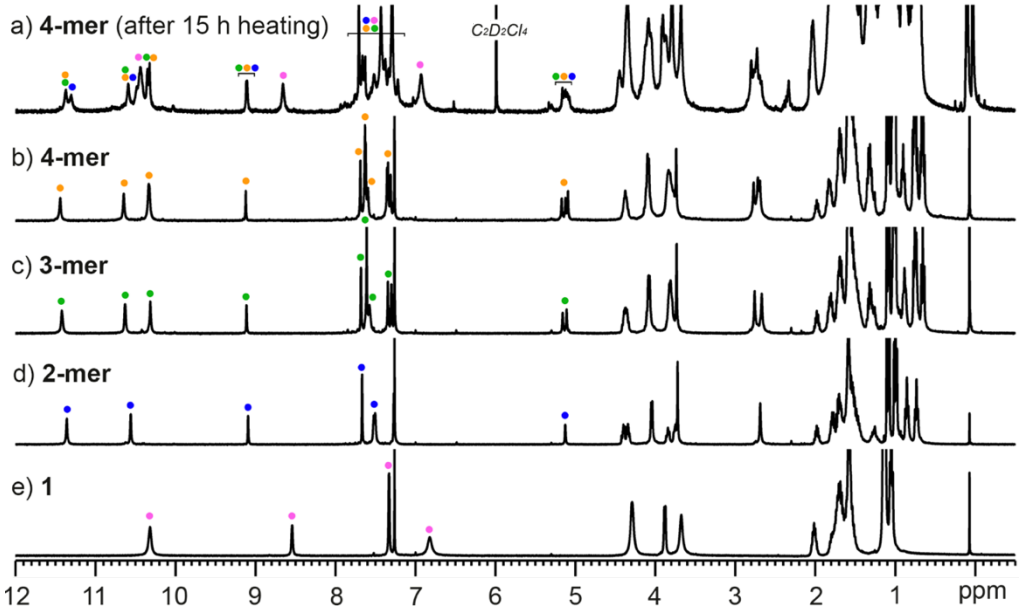

Fig. S39 Comparison of intermediate ^{1}H-NMR obtained after 15 h of heating of **4-mer** with **3-mer**, **2-mer**, and **1**. It shows the trace of these oligomers, thus establishing gradual conversion to the monomer **1**. The ^{1}H-NMR spectra for **1**, **2-mer**, **3-mer**, and **4-mer** were recorded in $CDCl_3$, and **4-mer** (after 15 h heating) was recorded in $C_2D_2Cl_4$ at 298 K.

Feeding experiment: Macrocycle **1** (10 mg) was dissolved in degassed $CDCl_3$ under N_2 atmosphere and then photoirradiated for one hour to generate a stock solution. Changes during the photoirradiation was monitored by ^1H NMR spectra. An aliquot was injected into a recycling GPC to estimate the amount of oligomers formed. To the stock solution, fresh 10 mg of 1 was added under a nitrogen atmosphere, and the mixture was subjected to further photoirradiation for another hour (Feeding-I). An aliquot was then injected in recycling GPC to measure the changes in the amount of oligomers compared to the stock solution. The same procedure was repeated for one more cycle (Feeding-II).

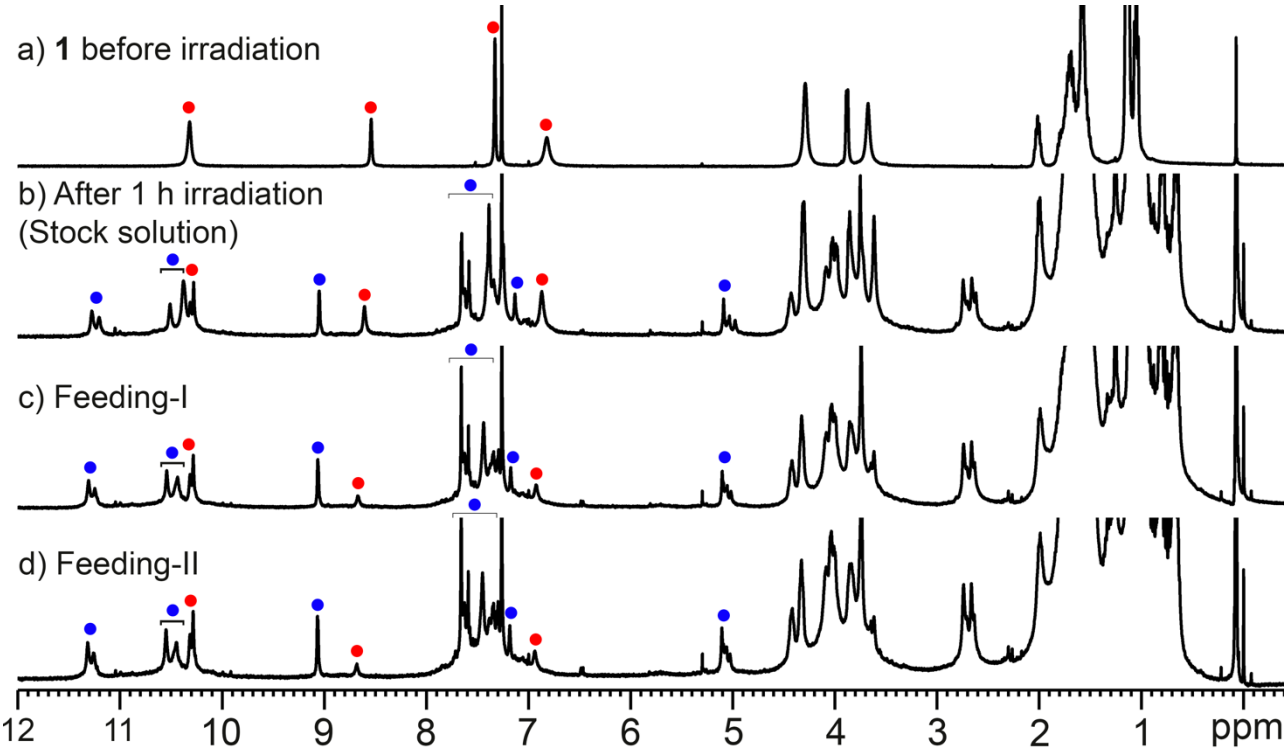

Fig. S40 Stacked 400 MHz ^1H-NMR plot of feeding process. (a) Macrocycle **1** before photoirradiation in $CDCl_3$ at 298 K. (b) After 60 min of photoirradiation to have a stock of oligomers. (c) After adding fresh **1** to stock solution and subsequent photoirradiation for 1 hour (Feeding-I). (d) After adding fresh **1** to the Feeding-I and photoirradiation for 60 mins (Feeding-II) in degassed $CDCl_3$ at 298K. The red and blue circles represent signals corresponding to **1**, and new peaks appeared through the irradiation process, respectively.

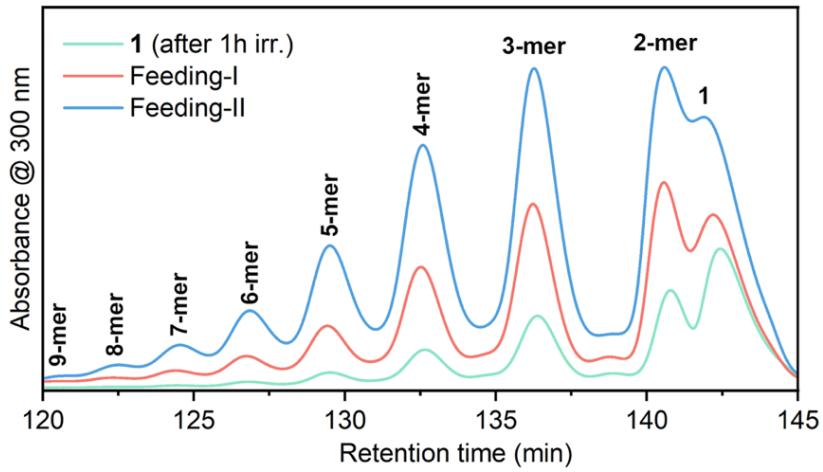

Fig. S41 Stacked recycling GPC profile after 4th cycle. **Stock:** photoirradiation of **1** for 1 h to get a stock solution (green line). **Feeding-I:** addition of fresh monomer **1** to the stock solution and photoirradiated for another 1 h (red line). **Feeding-II**: addition fresh **1** to **Feeding-I** and photoirradiated for 1 h again (Blue line).

Photooligomerization of 1 in the presence of 3-mer: Trimer and macrocycle **1** were mixed and dissolved in degassed $CDCl_3$ under N_2 atmosphere and the mixture was subjected to photoirradiation for 30 mins. Changes monitored through ^1H NMR and GPC technique. The evolution of oligomers was compared with if only macrocycle **1** photoirradiated for 30 mins.

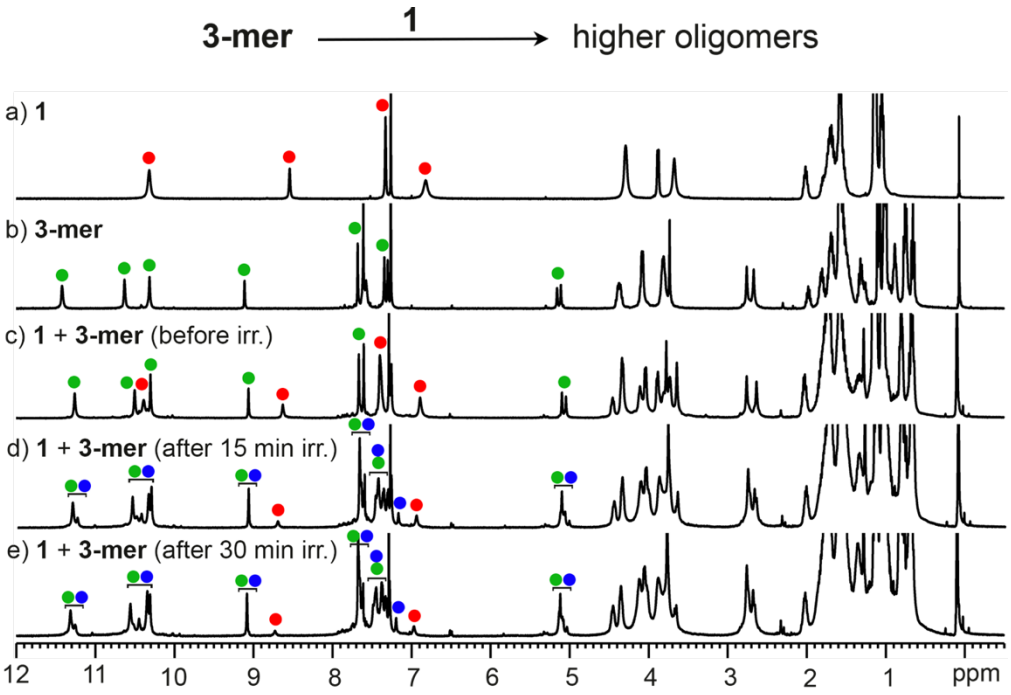

Fig. S42 Stacked ^1H NMR plot of a photooligomerization process when **1** was irradiated in the presence of **3-mer**. The 400 MHz ^1H-NMR of **1** (a), **3-mer** (b), and **1**+**3-mer** (c). The ^1H-NMR after photoirradiation of **1** and **3-mer** mixture for 15 min (d) and 30 min (e). All the experiments were performed in $CDCl_3$ under a nitrogen atmosphere at 298 K.

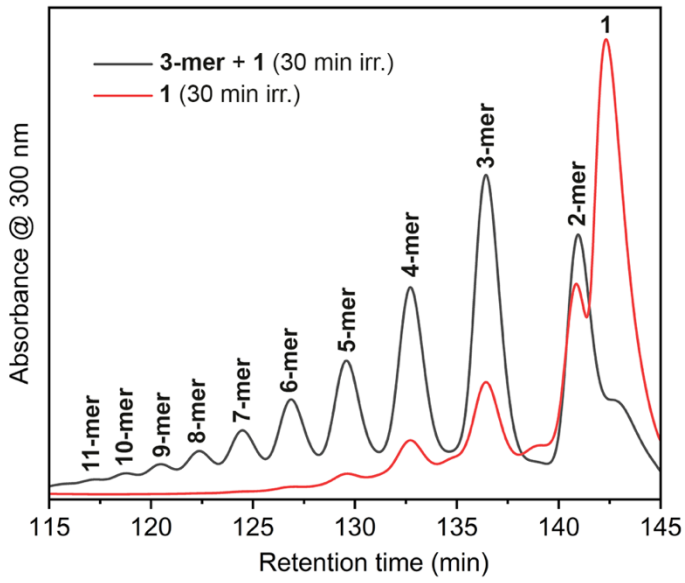

Fig. S43 Stacked recycling GPC profile after 4th cycle. After 30 mins photoirradiation of mixture of **3-mer** and **1** (black line). GPC profile after 4th cycle given as a reference for **1** when photoirradiated for 30 mins (red line).

Photoirradiation of 2-mer: To investigate whether a multiple of **2-mer** can form if **2-mer** is photoirradiation alone, 10 mg was dissolved in degassed $CDCl_3$ under an N_2 atmosphere and then subjected to photoirradiation for 30 mins. The evolution of oligomers is monitored through ^{1}H-NMR and GPC. It was compared with if macrocycle **1** photoirradiated for 30 mins.

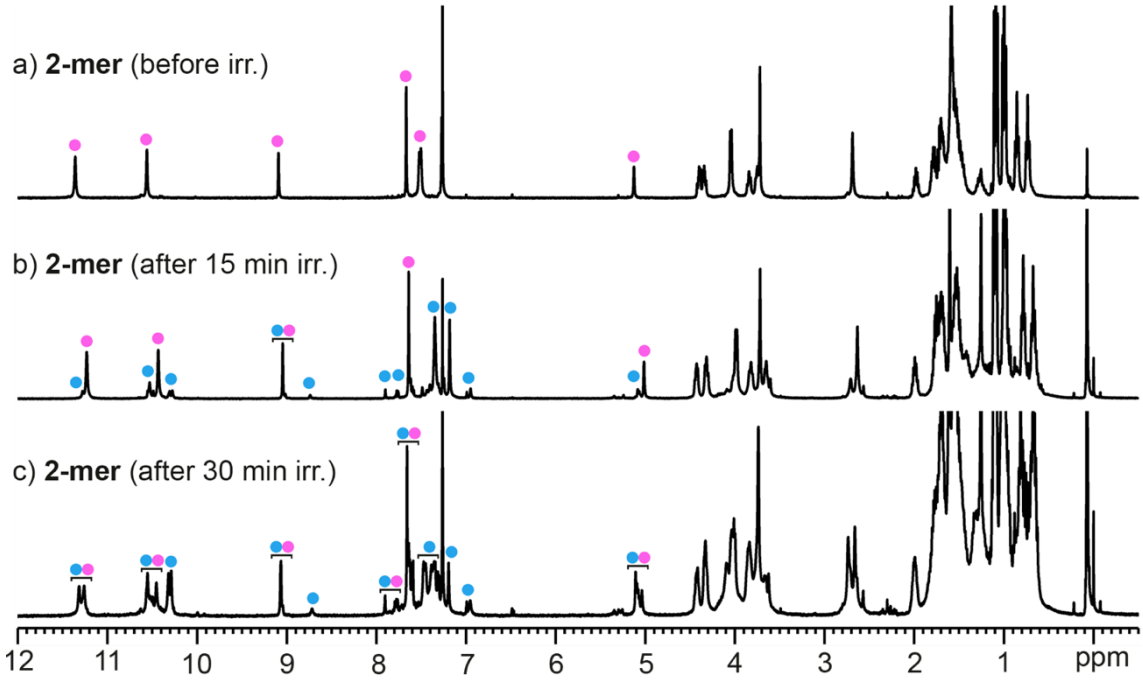

Fig. S44 Stacked 400 MHz ^{1}H-NMR plot of a photooligomerization process when **2-mer** was irradiated in degassed $CDCl_3$ at 298 K. The ^{1}H-NMR of **2-mer** before photoirradiation (a), after 15 min of photoirradiation (b), and after 30 min of photoirradiation (c).

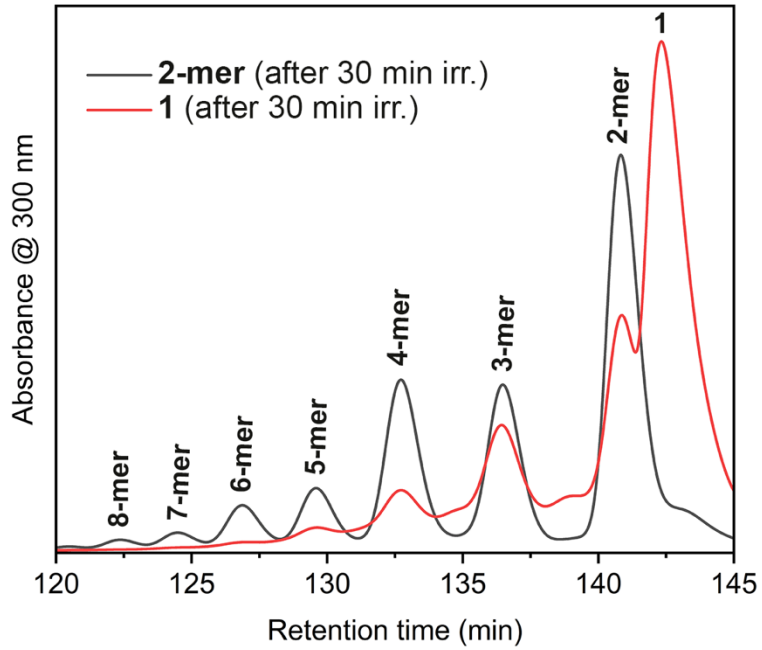

Fig. S45 Stacked recycling GPC profile after 4th cycle. After 30 mins photoirradiation of **2-mer** (black line). GPC profile after 4th cycle given as a reference for **1** when photoirradiated for 30 mins (red line).

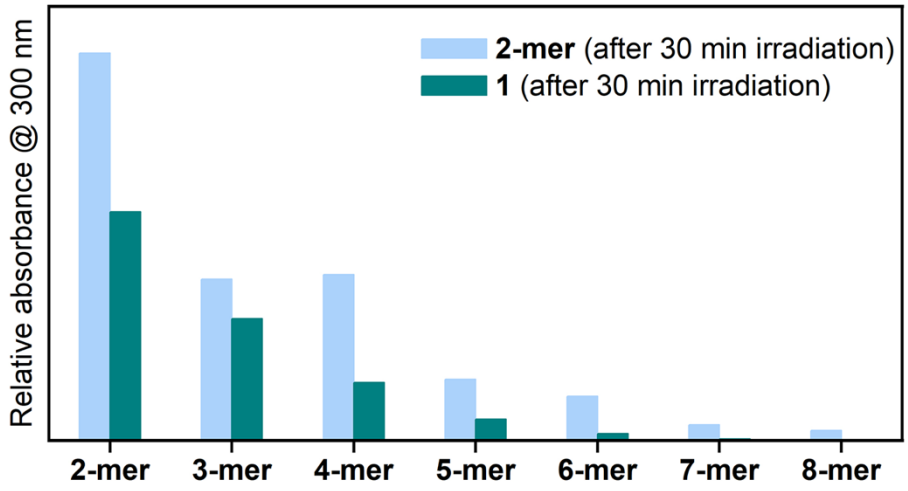

Fig. S46 The plot shows the evolution of different oligomers when a solution of **2-mer** was irradiated for 30 min (sky blue bar) compared with a photoirradiated solution of **1** (green bar). Note that the relative proportion of **4-mer**, **6-mer** etc. is higher when starting from a **2-mer** solution.

2. Material and methods

2.1 General information

All reactions were carried out under a dry, anaerobic atmosphere; it is specified otherwise. All Solvents and chemicals were purchased from Finar, Rankem, Sigma-Aldrich, TCI Chemicals, Alfa-Aesar, or BLD Pharma and were used without further purification. Tetrahydrofuran (THF) and dichloromethane (CH_2Cl_2) were dried over MBRAUN SPS-800 solvent purification system; chloroform ($CHCl_3$) and diisopropylethylamine (DIPEA) were distilled over P_2O_5 and calcium hydride (CaH_2) respectively before use. Reactions were monitored by thin layer chromatography (TLC) on Merck silica gel 60-F254 plates and observed under UV light. Column chromatography purifications were performed using silica gel (100-200 mess). Preparative recycling gel permeation chromatography (GPC) was performed on the Japan Analytical Industry (JAI) LaboACE LC-5060 instrument using JAIGEL-2HR and JAIGEL-2.5HR (20×600 mm) columns at a flow rate of 7 mL/min with a mobile phase composed of 1% (vol/vol) ethanol and 0.5% (vol/vol) Et_3N in chloroform. Monitoring was carried out by UV detector at 254 nm, 300 nm, 400 nm, and 500 nm.

2.2 Nuclear Magnetic Resonance

NMR spectra were recorded on an Avance III HD 400 NMR spectrometer (Bruker Biospin, Wissembourg, France) with a vertical 9.4 T narrow-bore/ultrashield magnet operating at 400 MHz for ^{1}H spectra and 100 MHz for ^{13}C spectra using a 5 mm Smartprobe BBFO $^{1}H/^{15}N$-^{31}P-^{19}F probe with Z gradient capabilities. Chemical shifts are reported in parts per million (ppm, δ) relative to the residual proton signal of the deuterated solvent used. The ^{1}H NMR splitting patterns with observed first-order coupling are designated as singlet (s), doublet (d), triplet (t), quartet (q), or multiplate (m). Coupling constants (*J*) are reported in hertz. Samples were not degassed; otherwise, it is specified. Data processing was performed with Bruker Topspin 3.6.4 software. Diffusion experiments (DOSY NMR) were performed at 298 K in $CDCl_3$. The diffusion coefficient was calculated after processing the experimental DOSY spectrum with the T1/T2 software. The diffusion coefficient for higher oligomers (**7-mer** onwards) cannot be measured due to their low solubility and high aggregation propensity. At lower concentrations (< 0.5 mM), reliable fitting and diffusion coefficient was not obtained.

2.3 Mass Spectroscopy

High-resolution ESI mass spectra (HR-MS) were recorded using Agilent 6540 UHD Accurate-Mass Q-TOF LC/MS system. MALDI-TOF mass spectra were recorded using Bruker Autoflex maX MALDI TOF/TOF instrument. The matrix used was α-Cyano-4-hydroxycinnamic acid (CHCA) and sinapic acid.

2.4 Spectroscopic studies

Electronic absorption spectra were measured on Agilent Technologies Cary 8454 UV-Vis spectrophotometer. All solvents used for spectrophotometric analysis were of analytical grade. The UV-vis spectroscopic measurements were carried out using ca. 10^{-6} M solutions of the macrocycle **1** in dichloromethane (DCM) in a 1 mm quartz cuvette.

2.5 Photochemistry

Photoirradiation experiments were carried out on sample solutions in NMR tubes. Respective compounds were placed in NMR tubes, degassed, and filled with nitrogen. Subsequently, nitrogen-purged deuterated solvent ($CDCl_3$) was used to dissolve the compounds. The solutions were then subjected to irradiation by OmniCure S1500 portable device with a light guide having a light source of 200 W mercury arc lamp. A filter was used to allow 320 – 390 nm light for the irradiation. The ^{1}H-NMR spectra were checked at different intervals to follow the photoproduct formation. The experiments were repeated several times to establish reproducibility.

2.6 Computational methods

The geometry optimizations of **1** were performed using hybrid DFT functional, B3LYP as implemented in the Gaussian 09 suite package, with a 6-31G basis set.[1-7] Frequency calculations are performed to estimate the ground state of these monomeric units. The absence of negative frequencies indicates minimum energy structures for these isomers.

The geometry optimizations of oligomers were not performed using DFT method due to their large size. Therefore, Molecular minimizations were done using MacroModel version 8.6 (Schrödinger Inc.) with the Merck Molecular Force Field static (MMFFs) as implemented in this software. Energy-minimized structures were obtained using 500 steps of Truncated Newton Conjugate Gradient (TNCG), chloroform as an implicit solvent, and the extended Cutoff option.

3. Methods for chemical synthesis

3.1 Synthetic procedures

Methyl 8-acetoxy-4,6-bis(2-ethylbutoxy)-10-methylpyrido[3,2-g]quinoline-2-carboxylate, 2. In a 100 mL round bottomed flask, diketo reactant[8] (5 g, 14.61 mmol, 1 eq) and triphenyl phosphine (9.6 g, 36.52 mmol, 2.5 eq) was dissolved in 60 mL of dry THF. To the mixture, 2-ethylbutan-1-ol (4.2 mL, 34.11 mmol, 2.3 eq) was added with constant stirring. The reaction mixture was cooled to 0 °C, and DIAD (7.2 mL, 36.67 mmol, 2.5eq) was added dropwise and stirred at 0 °C for 30 min and then at room temperature for 16 hours. After completion, the solvent was evaporated completely, and the residue was dissolved in a DCM-MeOH (1:1 ratio) mixture and kept in the fridge to crystallize. Crystals obtained were filtered and washed with cold MeOH and dried under vacuum to get **2** as yellow solid (6.62 g, 88%). ^{1}H NMR (400 MHz, $CDCl_3$) δ (ppm): 9.10 (s, 1H), 7.52 (s, 2H), 4.27 (d, J = 5.3 Hz, 4H), 4.10 (s, 6H), 3.50 (s, 3H), 1.94 – 1.86 (m, 2H), 1.72 – 1.59 (m, 8H), 1.04 (t, J = 7.5 Hz, 12H).^{13}C NMR (100 MHz, $CDCl_3$, 298 K) δ ppm: 166.64, 163.69, 149.95, 146.04, 139.31, 121.82, 113.64, 98.81, 71.22, 53.32, 41.24, 23.94, 13.21, 11.54. HRMS (ESI): m/z calcd for $C_{29}H_{38}N_2O_6$ $[M+H]^+$ 511.2803, Found 511.2824.

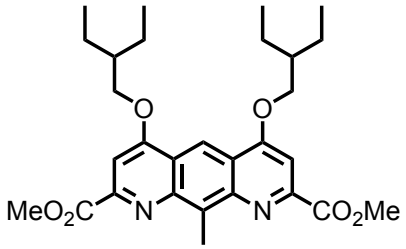

2

4,6-bis(2-ethylbutoxy)-10-methylpyrido[3,2-g]quinoline-2,8-dicarboxylic acid, 3. Diester **2** (2.15 g, 4.21 mmol, 1 eq) was dissolved in 100 mL DCM:MeOH (1:1 ratio) mixture in a 250 mL round bottom flask. In another 50 mL round bottom flask, KOH (709 mg, 12.63 mmol, 3 eq) was dissolved in 35 mL MeOH and added slowly to the earlier flask. The reaction mixture was stirred at room temperature for 24 hours. After completion, the solvent was evaporated completely. The yellow solid obtained was washed with 5% citric acid and then extracted with $CHCl_3$, and then washed with brine three times. The combined organic layer was dried over Na_2SO_4 and evaporated completely to get yellow product **3** (1.66 g, 82%). ^{1}H NMR (400 MHz, $CDCl_3$) δ (ppm): 9.19 (s, 1H), 7.64 (s, 2H), 4.32 (d, J = 5.4 Hz, 4H), 3.36 (s, 3H), 1.96 – 1.89 (m, 2H), 1.70 – 1.62(m, 8H), 1.04 (t, J = 7.5 Hz, 12H). ^{13}C NMR (100 MHz, $CDCl_3$, 298 K) δ ppm: 165.40, 164.44, 148.96, 144.37, 136.30, 122.24, 115.25, 97.03, 72.07, 41.14, 23.90, 12.94, 11.49. HRMS (ESI): m/z calcd for $C_{27}H_{34}N_2O_6$ $[M+H]^+$ 483.2490, Found 483.2488.

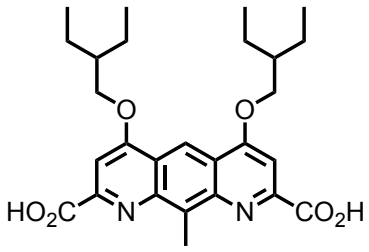

3

Dimethyl 4-(2-ethylbutoxy)pyridine-2,6-dicarboxylate, 4. In a round bottom flask, dimethyl 4-oxo-1,4-dihydropyridine-2,6-dicarboxylate[9] (4.1 g, 19.41 mmol, 1 eq) and triphenylphosphine (10 g, 38.12 mmol, 1.9 eq) were dissolved in 40 mL of dry THF. To the mixture, 2-ethylbutan-1-ol (3.6 mL, 29.24 mmol, 1.5 eq) was added with constant stirring. The reaction mixture was then cooled to 0 °C, and DIAD (7.4 mL, 38 mmol, 1.9 eq) was added dropwise. The mixture was stirred at 0 °C for 30 min and then at room temperature for 16 hours. After completion, the solvent was evaporated completely, and the residue obtained was purified by column chromatography (ethyl acetate/petroleum ether 20:80), and product **4** was obtained as a white solid (4.81 g, 84%). ^{1}H NMR (400 MHz, $CDCl_3$, 298 K) δ ppm: 7.81 (s, 2H), 4.03 (d, J = 5.7 Hz, 2H), 4.01 (s, 6H), 1.74-1.69 (m, 1H), 1.53-1.45 (m, 4H), 0.94 (t, J = 7.5 Hz, 6H). ^{13}C NMR (100 MHz, $CDCl_3$) δ 167.41, 165.34, 149.79, 114.66, 71.24, 53.31, 40.68, 23.32, 11.16. HRMS (ESI): m/z calcd for $C_{15}H_{21}NO_5$ $[M+H]^+$ 296.1492, Found 296.1482.

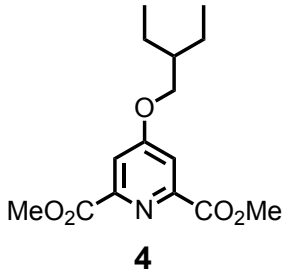

4

4-(2-ethylbutoxy)pyridine-2,6-dicarboxamide, 5. Ester **4** (3.4 g, 6.77 mmol, 1 eq) was dissolved in 45 mL dry MeOH. Dry NH_3 gas was gently purged into the solution for 2 hours at room temperature. The resulting white precipitate was filtered off, washed with MeOH, dried under vacuum, and used without further purification. (2.2 g, 72%). ^{1}H NMR (400 MHz, DMSO-d_6, 298 K) δ ppm: 8.83 (s, 2H), 7.70 (s, 2H), 7.65 (s, 2H), 4.08 (d, J = 5.9 Hz, 2H), 1.67-1.63 (m, 1H), 1.48-1.38 (m, 4H), 0.89 (t, J = 7.5 Hz, 6H). ^{13}C NMR (100 MHz, DMSO-d_6, 298 K) δ ppm: 167.19, 165.15, 151.17, 110.05, 70.50, 22.62, 10.81. HRMS (ESI): m/z calcd for $C_{13}H_{19}N_3O_3$ $[M+H]^+$ 266.1499, Found 266.1472

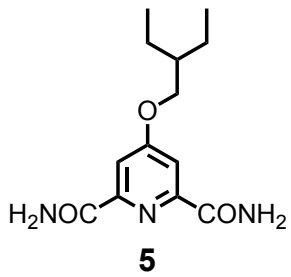

5

4-(2-ethylbutoxy)pyridine-2,6-diamine, 6. In a 250 mL round bottom flask, KOH (7.61 g, 135.63 mmol, 18 eq) was dissolved in 15 mL H_2O, and then 25 g of ice was added. Then Br_2 solution (1 mL, 19.41 mmol, 2.5 eq) was added slowly with constant stirring. After 10 mins, **5** (2 g, 7.53 mmol, 1 eq) was added, followed by the addition of 40 ml 1,4-dioxane. The reaction mixture was stirred at 0 °C for 10 mins, then 1 hour at 25 °C, and finally 1.5 hours at 70 °C. At this point, acetic acid (6 mL) was added, and after 30 mins, the reaction mixture was cooled to room temperature, and then 4 g of KOH was added. The resulting solution was extracted with DCM, washed with brine, and dried over Na_2SO_4. The crude product was purified by column chromatography (MeOH/Ethyl acetate 5:95) to yield a light brown solid (1 g, 64%). ^{1}H NMR (400 MHz, $CDCl_3$, 298 K) δ ppm:

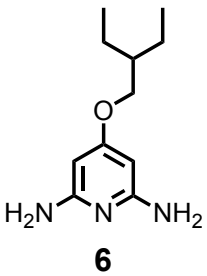

6

5.47 (s, 2H), 4.16 (s, 4H), 3.81 (d, J = 5.8 Hz, 2H), 1.63-1.58 (m, 1H), 1.46-1.38 (m, 4H), 0.91 (t, J = 7.5 Hz, 6H). ^{13}C NMR (100 MHz, $CDCl_3$, 298 K) δ ppm: 170.16, 157.11, 84.51, 70.40, 40.82, 23.46, 11.21. HRMS (ESI): m/z calcd for $C_{11}H_{19}N_3O$ $[M+H]^+$ 210.1601, Found 210.1616.

Macrocycle 1: Macrocycle **1** was prepared with a similar literature procedure.[10] Diazaanthracene diacid **5** (203 mg, 0.420 mmol, 1 eq) was dissolved in 6 mL dry $CHCl_3$. The solution was placed in an ice bath, and oxalyl chloride (0.36 mL, 4.2 mmol, 10 eq) was added dropwise. The reaction mixture was stirred at room temperature for 1.5 hours. After completion, the solvent was evaporated completely under a high vacuum for 3 hours. The acid chloride formed was used as it is for further reaction. The acid chloride was dissolved in 5 mL dry THF. In another 25 mL flask, diaminopyridine, **9** (88 mg, 0.42 mmol, 1 eq) was dissolved in 10 mL dry THF, and DIPEA (0.36 mL, 2.1 mmol, 5 eq) was added dropwise. This mixture was then added dropwise to the acid chloride solution in dry THF while maintaining the temperature at 0 °C. The reaction was stirred at 0 °C for 30 min and then at room temperature for 16 hours. After completion, the solvent was evaporated to dryness, and the residue was dissolved in $CHCl_3$. Washed with 5% citric acid, then with brine a few times. Finally, the organic fraction was dried over anhydrous Na_2SO_4. The solvent evaporated completely to get yellow crude. It was first passed through a silica gel column and then purified by gel permeable chromatography to get a bright yellow solid (180 mg, 33%). ^{1}H NMR (400 MHz, $CDCl_3$, 298 K) δ ppm: 10.32 (s, 4H), 8.54 (s, 2H), 7.33 (s, 4H), 6.82 (s, 4H), 4.30 (s, 8H), 3.88 (d, J = 6.4 Hz, 4H), 3.67 (s, 6H), 2.00-1.98 (m, 6H), 1.81 – 1.64 (m, 24H), 1.13 (t, J = 7.6 Hz, 24H), 1.04 (t, J = 7.5 Hz, 12H). ^{13}C NMR (100 MHz, $CDCl_3$, 298 K) δ ppm: 168.42, 164.29, 161.15, 150.02, 149.00, 144.24, 136.35, 121.03, 113.53, 95.42, 94.18, 71.81, 70.97, 41.10, 23.75, 23.34, 11.51, 11.38, 1.16, 0.13. MALDI-TOF: m/z calculated for $C_{76}H_{98}N_{10}O_{10}$ $[M+H]^+$ 1311.75, Found 1311.94.

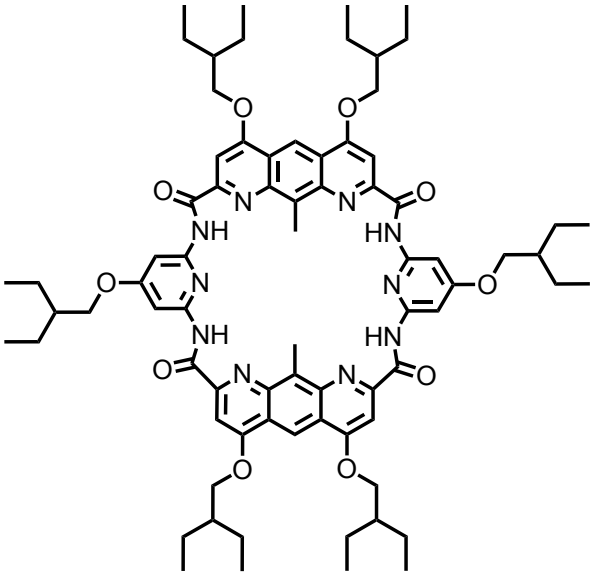

1

Photo-oligomerization of 1: Macrocycle **1** (15 mg) was dissolved in degassed $CDCl_3$ (0.5 mL) under N_2 atmosphere and then photoirradiated with 320-390 nm light for 3 hours. Then, the different oligomers were separated by the recycling GPC. The isolated yield of the different oligomers is as follows. **2-mer** (4.6 mg, 30%), **3-mer** (3.8 mg, 26%), **4-mer** (2.4 mg, 18%), **5-mer** (1.4 mg, 10%), **6-mer** (0.8 mg, 6%), **7-mer** (0.3 mg, 2%), **8-mer** (0.05 mg, 1.3%).

4. References

1. Gaussian 09, Revision A.02, M. J. Frisch *et. al.* Gaussian, Inc., Wallingford CT, 2016.
2. A. D. Becke, *J. Chem. Phys.,* 1993, **98**, 5648.
3. C. Lee, W. Yang and R. G. Parr, *Phys. Rev. B,* 1988, **37**, 785.
4. R. Ditchfield, W. J. Hehre and J. A. Pople, *J. Chem. Phys.,* 1971, **54**, 724.
5. P. C. Hariharan and J. A. Pople, *Theor. Chim. Acta,* 1973, **28**, 213.
6. W. J. Hehre, R. Ditchfield and J. A. Pople, *J. Chem. Phys.,* 1972, **56**, 2257.
7. V. A. Rassolov, J. A. Pople, M. A. Ratner and T. L. Windus, *J. Chem. Phys.,* 1998, **109**, 1223.
8. M. L. Singleton, N. Castellucci, S. Massip, B. Kauffmann, Y. Ferrand, I. Huc, *J. Org. Chem.* 2014, **79**, 2115–2122.
9. B. N. Ahamed, R. Duchene, K. Robeyns, C. A. Fustin, *Chem. Commun.* 2016, **52**, 2149–2152.
10. E. Berni, C. Dolain, B. Kauffmann, J. M. Leger, C. Zhan, I. Huc, *J. Org. Chem.* 2008, **73**, 2687–2694.

5. NMR Spectra

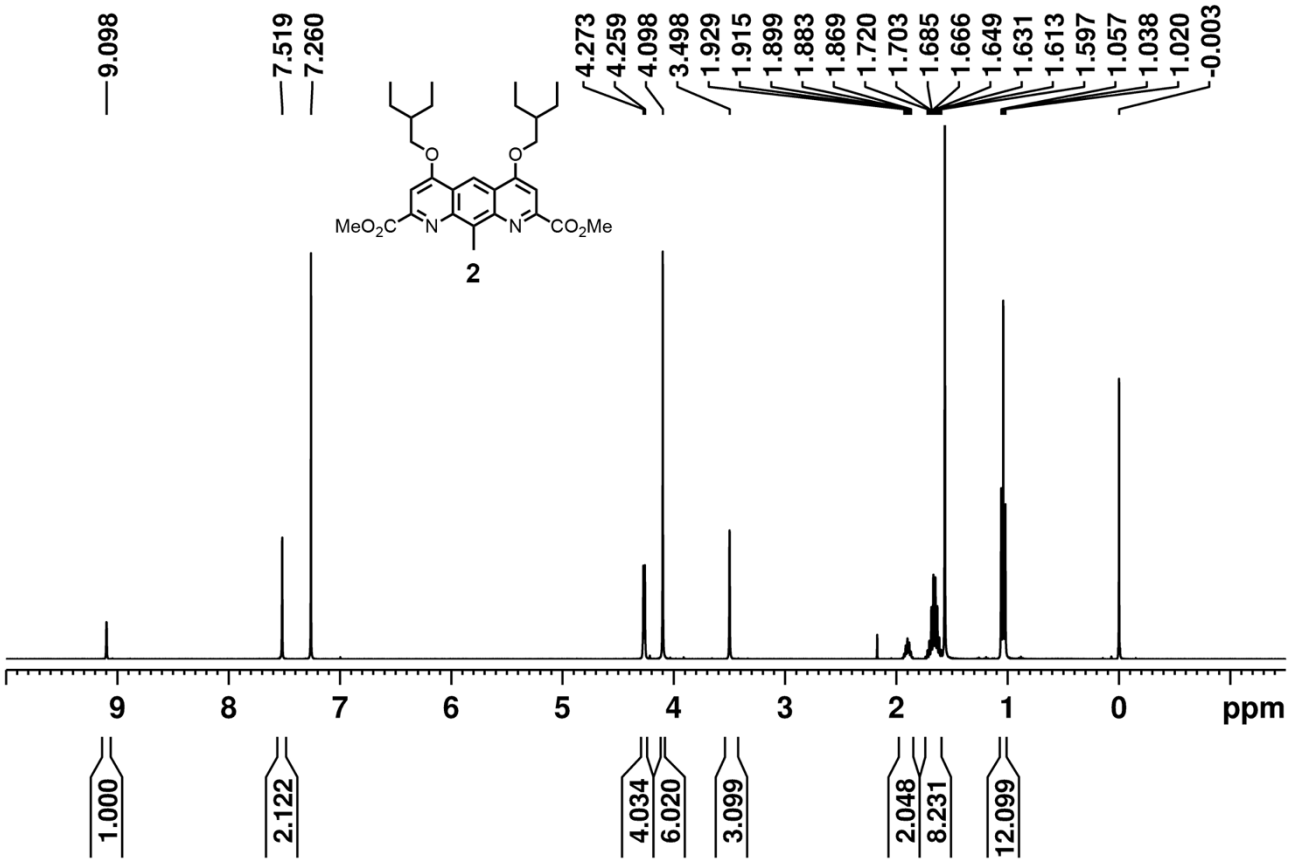

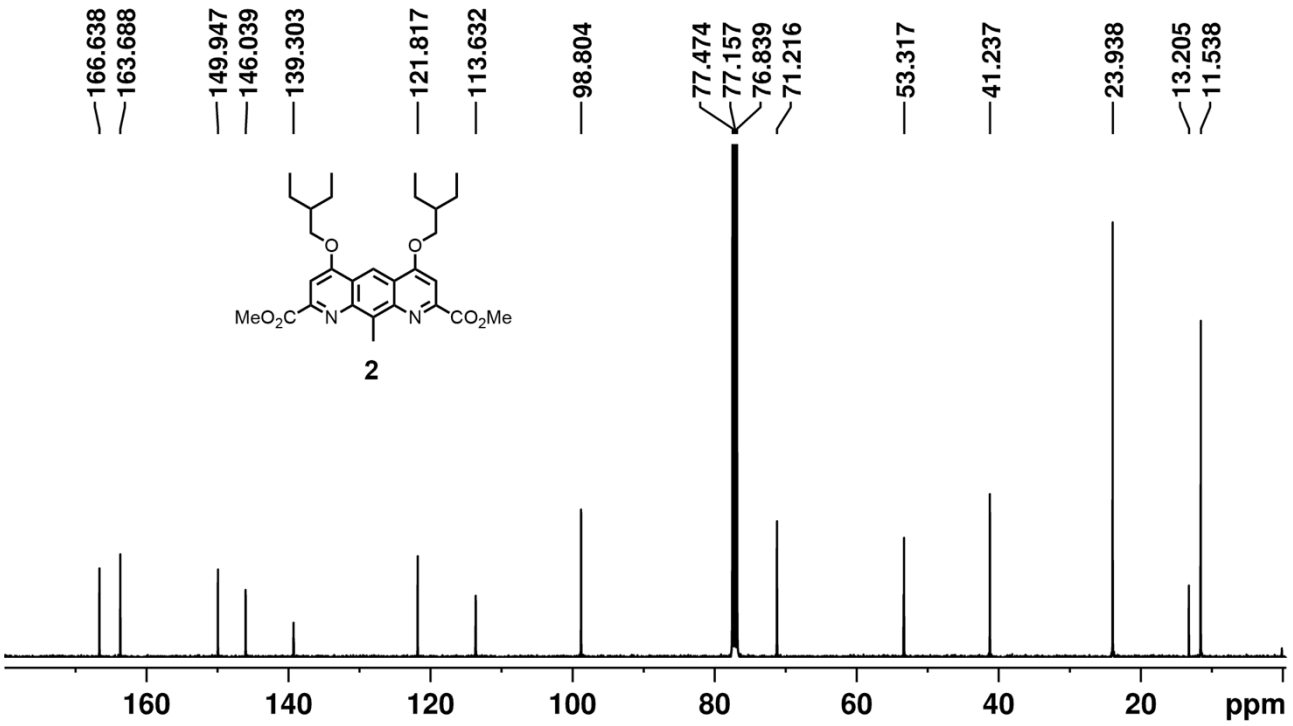
166.638
163.688
149.947
146.039
139.303
121.817
113.632
98.804
77.474
77.157
76.839
71.216
53.317
41.237
23.938
13.205
11.538
MeO2C
CO2Me
2
160
140
120
100
80
60
40
20
ppm

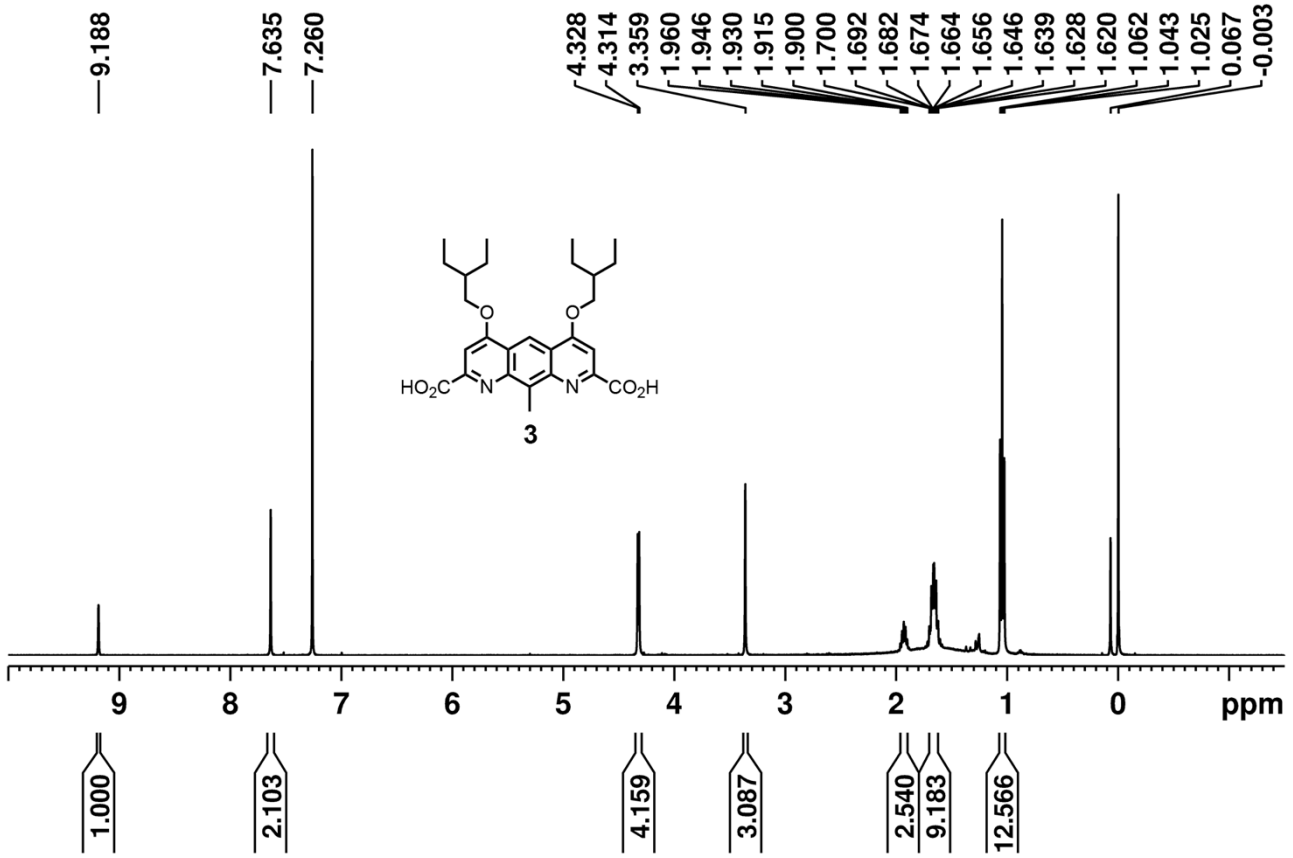
9.188
7.635
7.260
4.328
4.314
3.359
1.960
1.946
1.930
1.915
1.900
1.700
1.692
1.682
1.674
1.664
1.656
1.646
1.639
1.628
1.620
1.062
1.043
1.025
0.067
-0.003
HO2C
CO2H
3
9
8
7
6
5
4
3
2
1
0
ppm
1.000
2.103
4.159
3.087
2.540
9.183
12.566

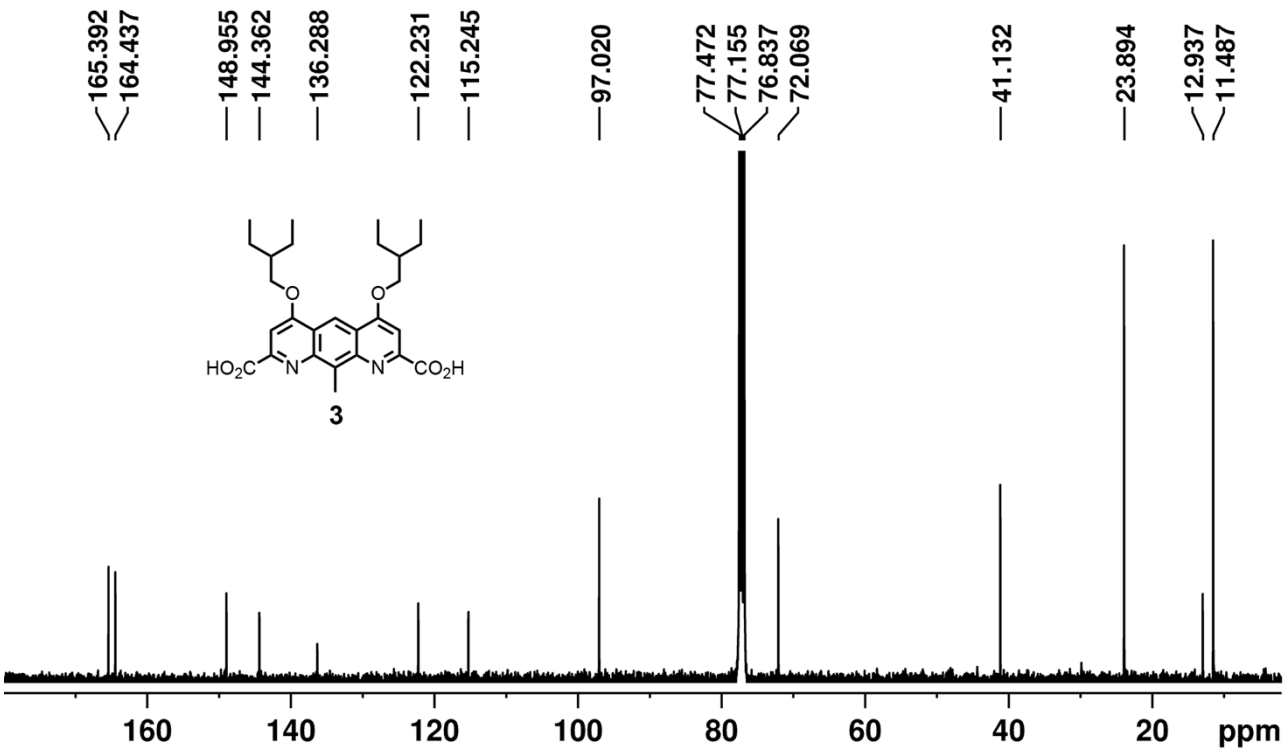
165.392
164.437
148.955
144.362
136.288
122.231
115.245
97.020
77.472
77.155
76.837
72.069
41.132
23.894
12.937
11.487
HO2C
N
N
CO2H
3
160
140
120
100
80
60
40
20
ppm

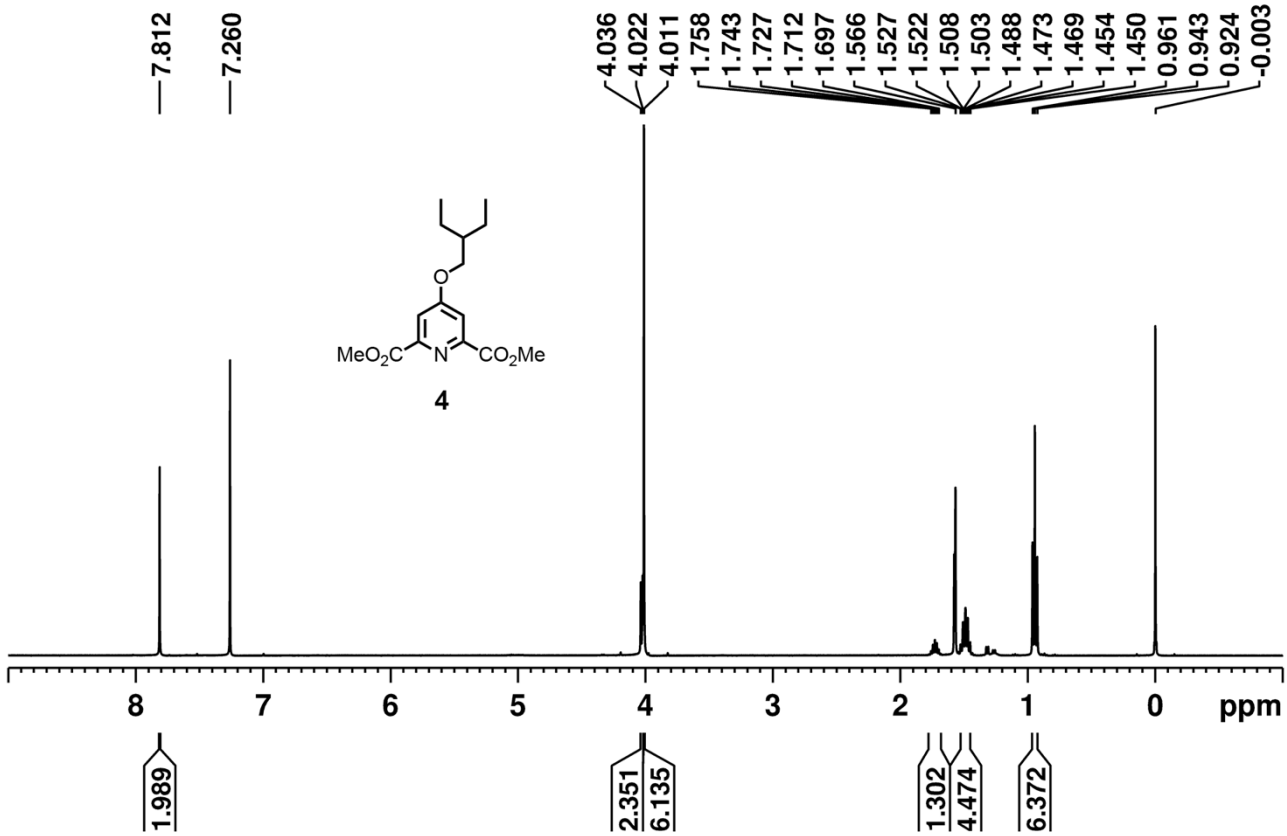
7.812
7.260
4.036
4.022
4.011
1.758
1.743
1.727
1.712
1.697
1.566
1.527
1.522
1.508
1.503
1.488
1.473
1.469
1.454
1.450
0.961
0.943
0.924
-0.003
MeO2C
N
CO2Me
4
8
7
6
5
4
3
2
1
0
ppm
1.989
2.351
6.135
1.302
4.474
6.372

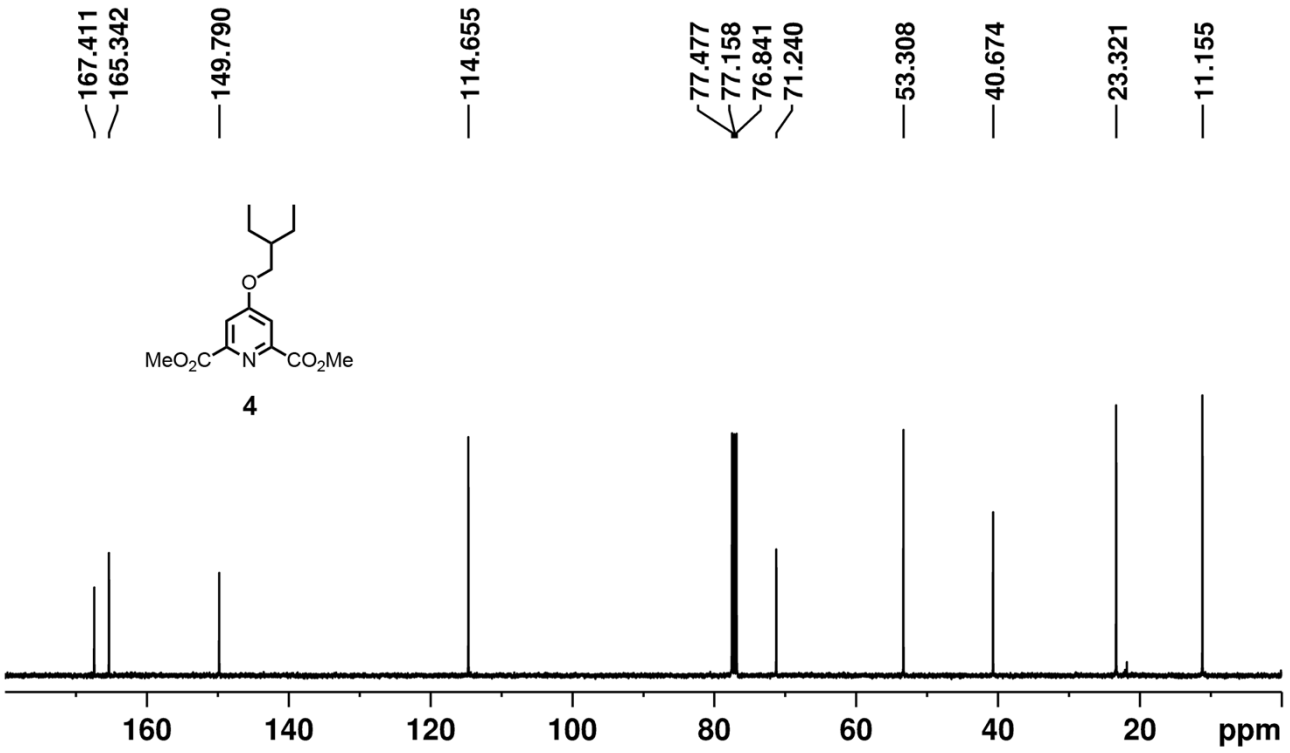
167.411
165.342
149.790
114.655
77.477
77.158
76.841
71.240
53.308
40.674
23.321
11.155
MeO2C
N
CO2Me
4
160
140
120
100
80
60
40
20
ppm

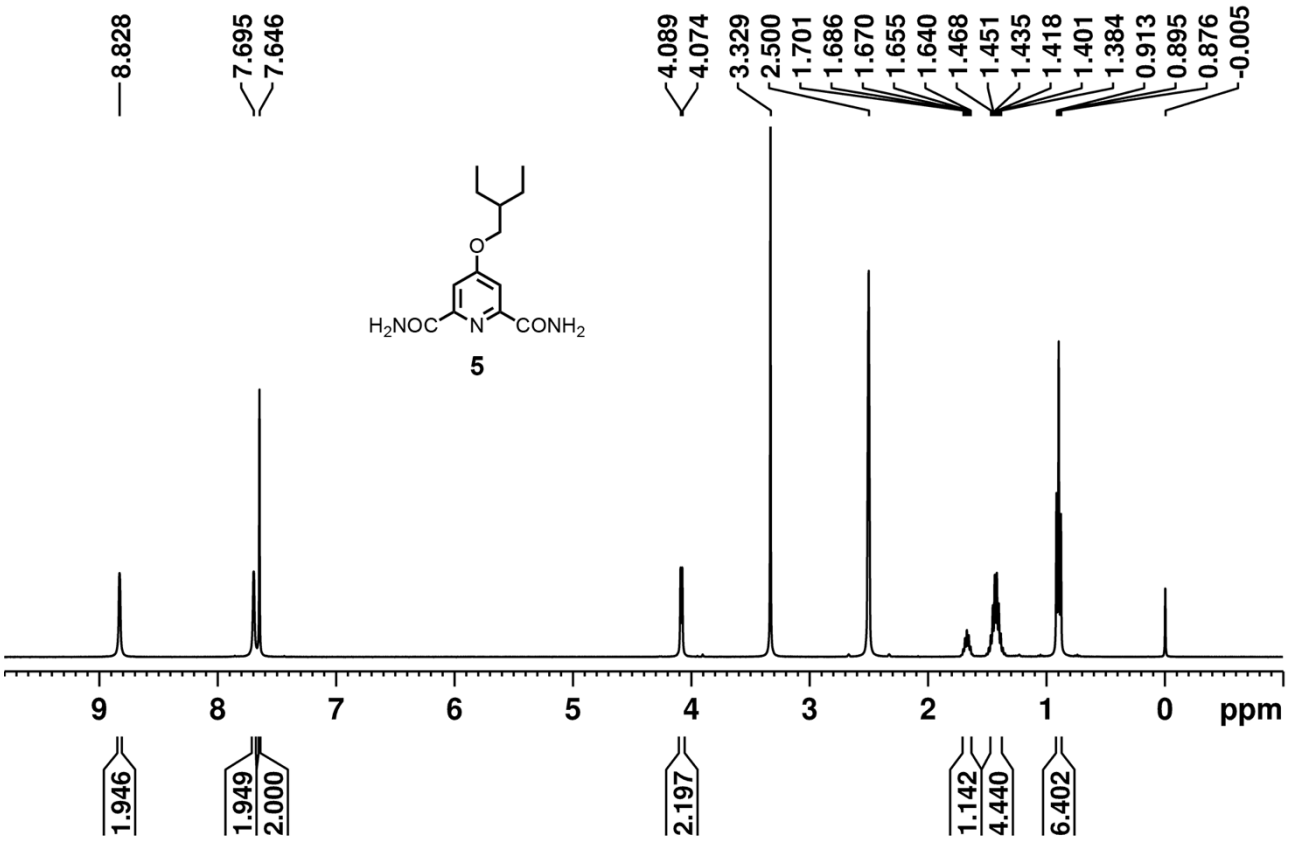
8.828
7.695
7.646
4.089
4.074
3.329
2.500
1.701
1.686
1.670
1.655
1.640
1.468
1.451
1.435
1.418
1.401
1.384
0.913
0.895
0.876
-0.005
H2NOC
N
CONH2
5
9
8
7
6
5
4
3
2
1
0
ppm
1.946
1.949
2.000
2.197
1.142
4.440
6.402

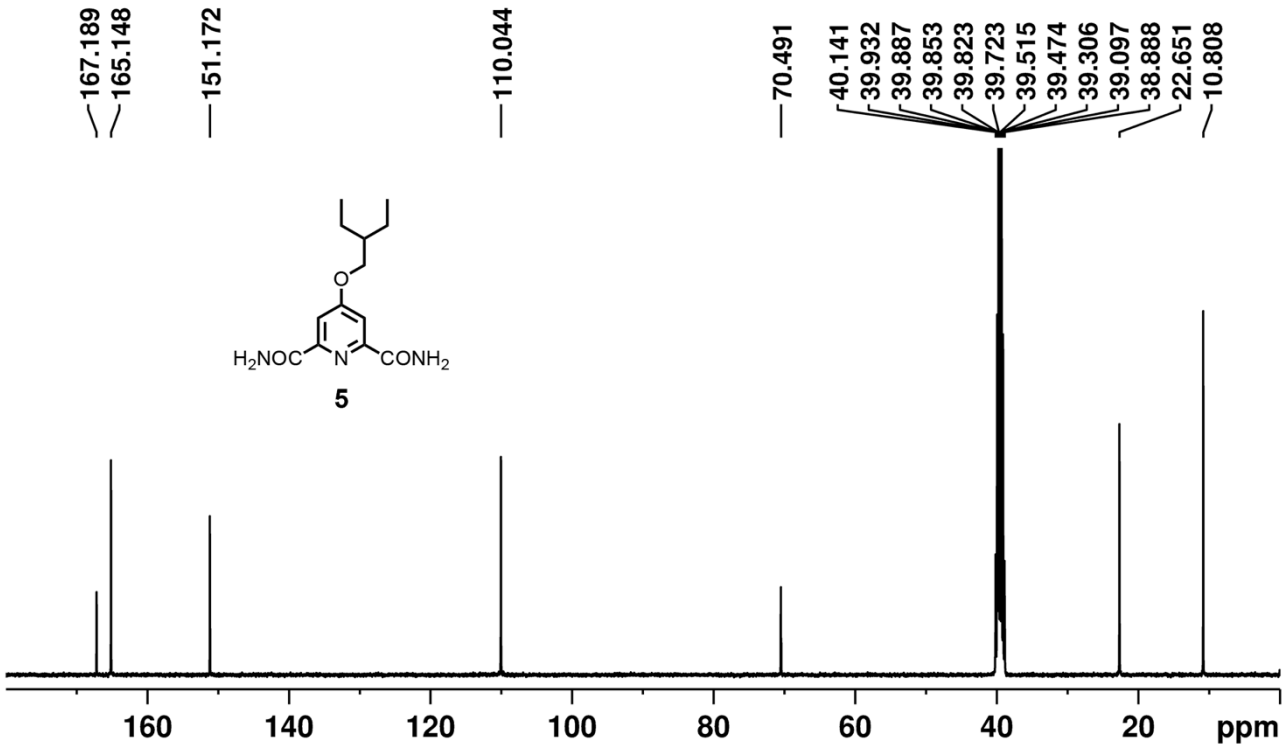
167.189
165.148
151.172
110.044
70.491
40.141
39.932
39.887
39.853
39.823
39.723
39.515
39.474
39.306
39.097
38.888
22.651
10.808
H2NOC
N
CONH2
5
160
140
120
100
80
60
40
20
ppm

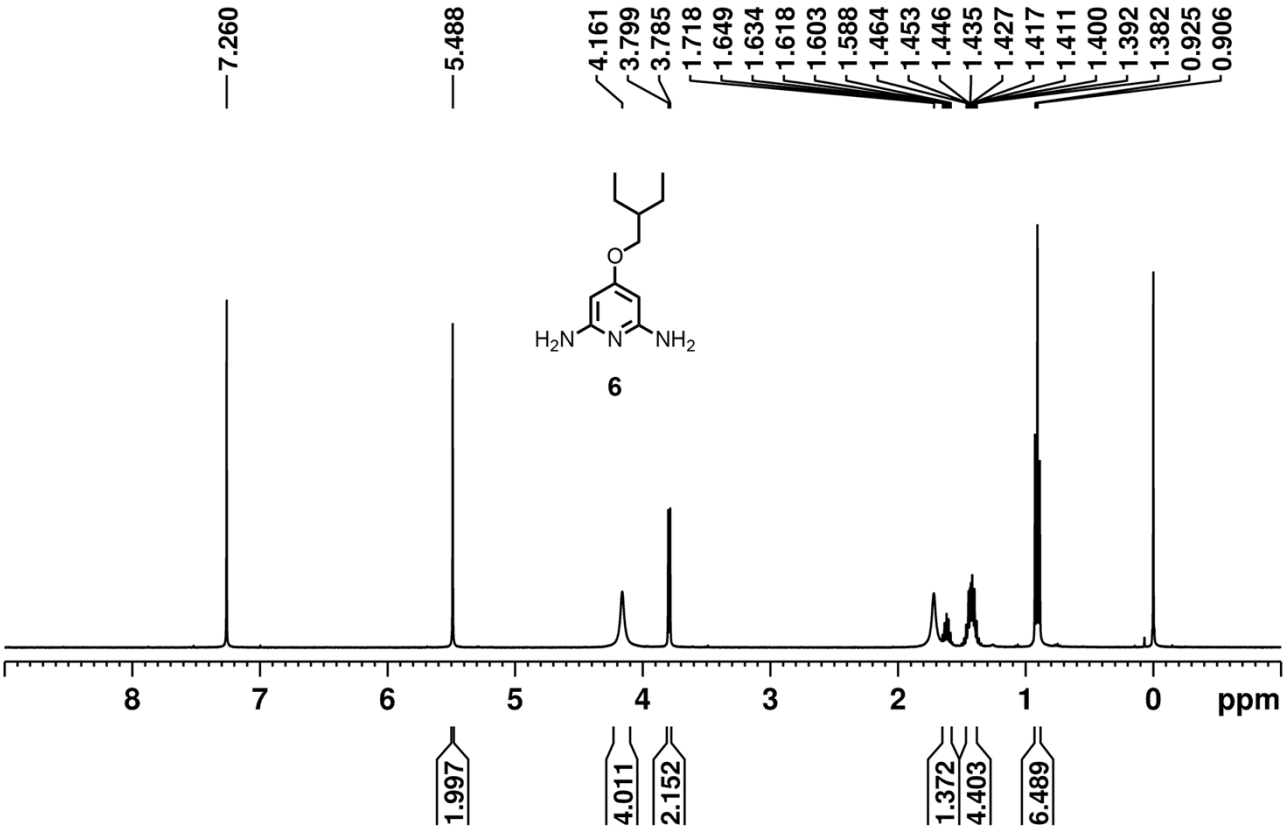
7.260
5.488
4.161
3.799
3.785
1.718
1.649
1.634
1.618
1.603
1.588
1.464
1.453
1.446
1.435
1.427
1.417
1.411
1.400
1.392
1.382
0.925
0.906
H2N
N
NH2
6
8
7
6
5
4
3
2
1
0
ppm
1.997
4.011
2.152
1.372
4.403
6.489

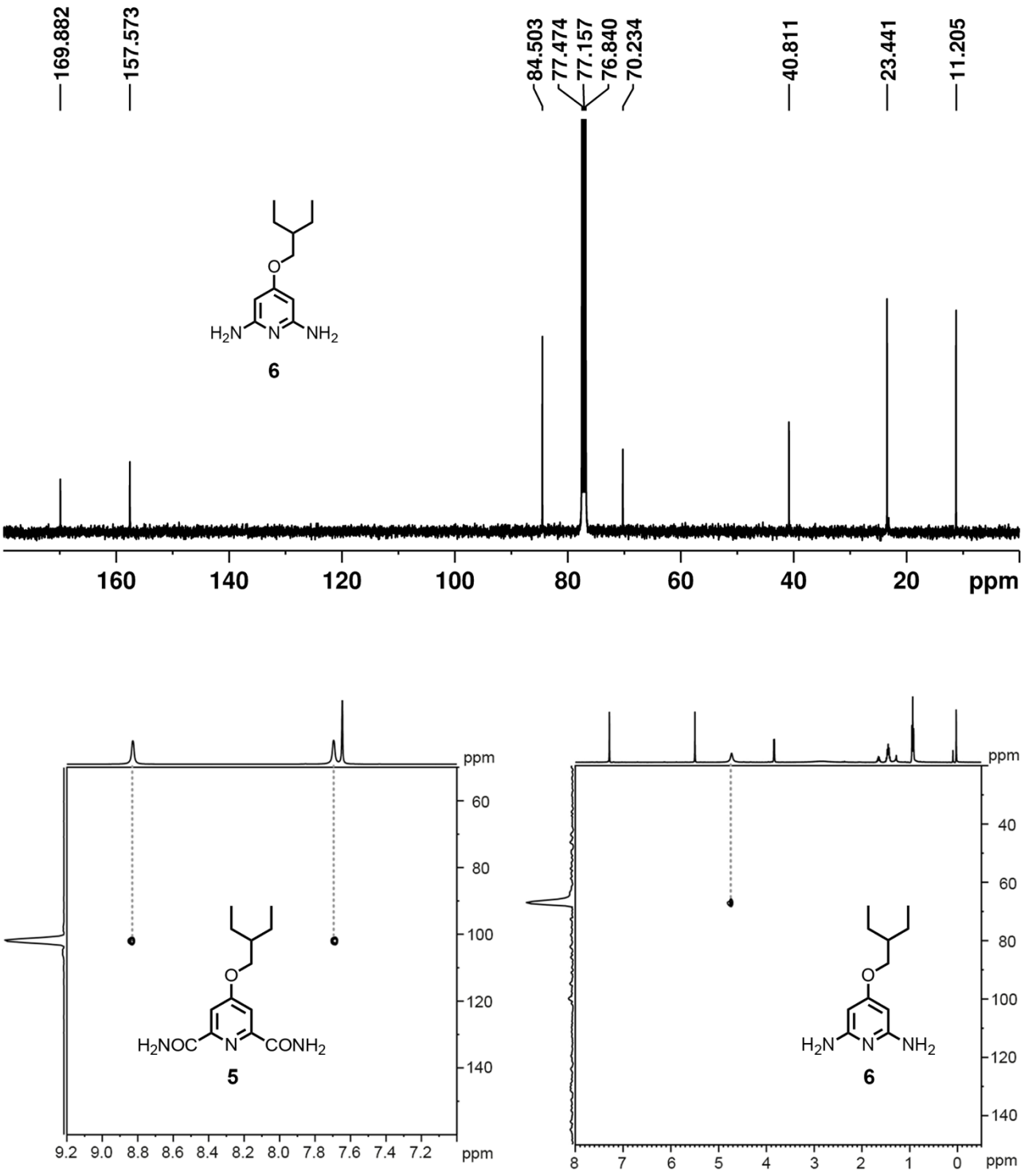

^{1}H-^{15}N HSQC for **8** and **9**.

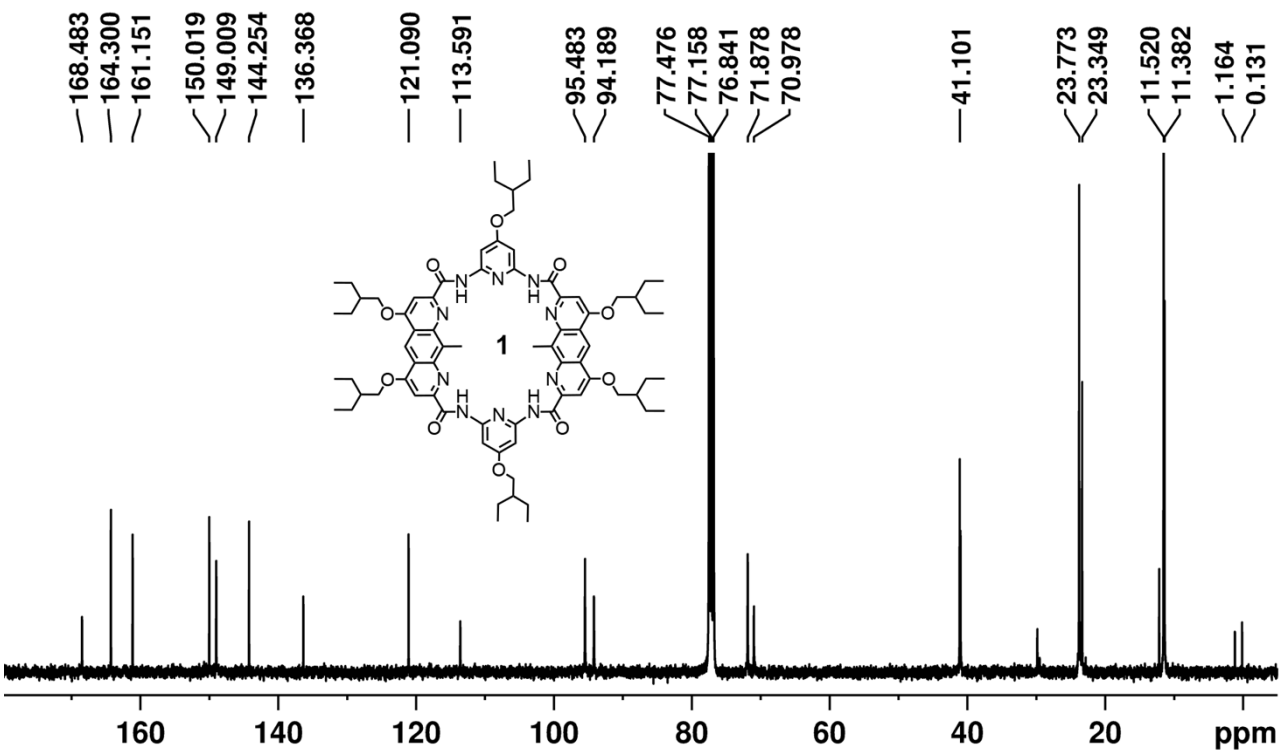
168.483
164.300
161.151
150.019
149.009
144.254
136.368
121.090
113.591
95.483
94.189
77.476
77.158
76.841
71.878
70.978
41.101
23.773
23.349
11.520
11.382
1.164
0.131
1
160
140
120
100
80
60
40
20
ppm